Maria Teresa Pinorini,[1] Ph.D.; Christopher James Lennard,[1] Ph.D.; Pierre Margot,[1] Ph.D.; Isabelle Dustin,[2] Ph.D.; and Patrick Furrer,[2] B.Sc.

Soot As an Indicator in Fire Investigations: Physical and Chemical Analyses

ABSTRACT: The possibility of determining the combustion products (or accelerants) at the seat of a fire by the analysis of corresponding soot samples was investigated. Twenty liquid fuels (principally petroleum derivatives) and twelve plastic materials (from seven different polymer groups) were individually burned over one hour under controlled laboratory conditions. The soot produced was collected on glass plates and subsequently submitted to a sequence of physical and chemical analyses. Twelve casework samples (soot deposits on glass fragments collected at the fire scene) and five control samples (blind trials prepared in the laboratory) were submitted to the same analytical procedure. A total of 49 soot samples were considered.

Macroscopic (35× magnification) and microscopic (TEM) studies were conducted on each soot sample. Digitized micrographs were processed in order to obtain certain physical parameters serving to characterize the size and form of the soot aggregates: perimeter, surface area, circularity and principal surface moments ratio. These data were transformed and used as variables for a discriminant analysis carried out with an SPSS program. Furthermore, the soot aggregates were characterized by their fractal dimension.

The chemical composition of the soot samples was explored using three chromatographic methods: GC-FID, GC-MS, and pyrolysis-GC. Two studies were conducted: a comparison of the total chromatographic profiles obtained by GC-FID and pyrolysis-GC, and a comparison based upon qualitative and semi-quantitative analyses of 11 polycyclic aromatic hydrocarbons (PAH's) in order to determine the value of these compounds as potential markers for accelerants used at the start of a fire.

The combination of physical and chemical parameters permitted the differentiation of most of the laboratory-prepared soot samples. The discriminating power was higher for the chemical analyses, with soot samples resulting from the combustion of plastic materials being the easiest to identify. Microscopy nevertheless provided interesting information concerning specific soot forms or elements. The combined results obtained by the analytical methods employed permitted the construction of a dichotomic table that can be used for the classification of soot samples taken from the scene of a fire. Additional research is required before such techniques can be routinely applied in casework.

A fire may be caused by natural, accidental or criminal means. In most arson cases, use is made of a product serving to initiate the fire or to facilitate its propagation; the term "accelerant" is used to designate a product of this type. The most common accelerants are liquid flammables or combustibles, often derived from petroleum. Analytical methods have been developed in order to identify such products extracted from the carbonized debris at the fire scene.

Concentration and analytical techniques by adsorption onto active charcoal (or porous polymer absorbants) followed by capillary gas chromatography are the most efficient at the present time and, under ideal conditions, permit the isolation and identification of extremely small quantities of accelerant [1]. However, at least three factors can influence the results obtained from such an analysis of accelerant residues:

a) the way in which the samples have been chosen, packaged and preserved [2];

b) the presence of materials (particularly petroleum-derived plastics, eg. polyester carpet, foam padding, etc. . .) which produce pyrolysis products that interfere with the identification of common accelerants including petroleum distillates and synthetic mixtures such as paint thinners and solvents [3];

c) the type of fire: during major destruction (for example, when the fire is particularly violent and/or prolonged), the combustibles at the source are destroyed and their isolation and identification from totally or partially carbonized debris is rendered uncertain, if not impossible.

In difficult cases, could the soot, which is always present in the case of incomplete combustion, be an exploitable medium for the search and identification of the burnt combustibles, particularly the accelerants?

In its formation, soot is preferentially deposited on cold spots, particularly on glass and metal surfaces; it therefore contains precious information on the materials burnt at the seat of the fire [4]. Soot aggregates are composed of sub-units or "elementary particles" (e.p.) which may be nearly spherical with a diameter which can vary between 5 and 250 nm, but is generally of the order of 20 to 30 nm (roughly 10^6 carbon atoms). In the case of building fires, the soot can be recovered from window panes or from glass fragments, particularly those resulting from thermal fracture due to the rise in temperature. Glass fragments may form in such a manner that they fall away from the building where they will no longer be affected by the fire [4]. Such glass samples may therefore be collected on the fringe of the fire scene and carry soot that was formed during the early stages of the fire.

Physical Analysis of Soot

With the aid of a transmission electron microscope, Arora [5] was able to show that soot, formed from the combustion of gasoline, kerosene, methylated spirits, charcoal, wood, cotton and paper, under controlled conditions of combustion and cooling, had distinct morphologic properties. According to this author, the transmission electron microscope permits the observation of specific properties such as size, form, internal structure, crystalline state, type of aggregation, and numerical density of the elementary particles. These characteristics allow the association of an unknown soot sample with the original combustible. The electron microscope has also been employed by various workers [6–8] for the measurement

and analysis of the physical characteristics of particles resulting from various combustion processes, particularly from diesel emissions.

It is known that structures comparable to those of soot aggregates have a "fractal dimension" varying between 1.7 and 1.9 [9]. The term "fractal" was invented by the French mathematician Mandelbrot around 1967 [10]. Fractal geometry is today an important tool for the description of objects where the structure remains similar no matter what magnification is considered. In particular, fractals have been used for the study of numerous random phenomena (chaos). The applications may be as varied as percolation, Brownian motion, the branching of nerve endings, or the structure of aggregates formed from nearly identical base units as is the case with soot. There exist structures such as, for example, Sierpinski's "carpet" (Fig. 1) which cannot be described by whole dimensions, but may be characterized by an intermediate, non-integer dimension: a *fractal* dimension (or Hausdorff dimension) [11].

If an object can be divided into N copies of itself, at a scale F, then the equation

$$N = \left(\frac{1}{F}\right)^{D}$$

is satisfied where D is the fractal dimension. This value can be obtained directly by taking the logarithm:

$$D = \frac{\ln (N)}{\ln (1/F)}$$

Chemical Analysis of Soot

The principal constituent of soot is without doubt carbon (> 90% by weight), but soot normally contains up to 6% oxygen and from 1 to 3 % hydrogen (up to 12% hydrogen by number of atoms), even more if the soot is sampled in the early stages of combustion. In fact, the atomic ratio C/H increases up to a factor of 8 times if the soot is aged in a flame [12].

Apart from the supporting carbon structure, soot particles may be characterized by the presence of: a) inorganic materials such as salts, oxides, metals, absorbed liquids and gases (particularly water) and sulfur and nitrogen based compounds; b) components which may be extracted from the soot by means of an organic solvent [also known as the "soluble organic fraction" (SOF)], composed of various classes of compounds, the majority being polycyclic aromatic hydrocarbons (PAH's), their derivatives and heterocyclic analogues; c) insoluble carbonaceous materials, generally resins, present in the form of a coating, binder or separate entity, or incompletely burnt fragments [13].
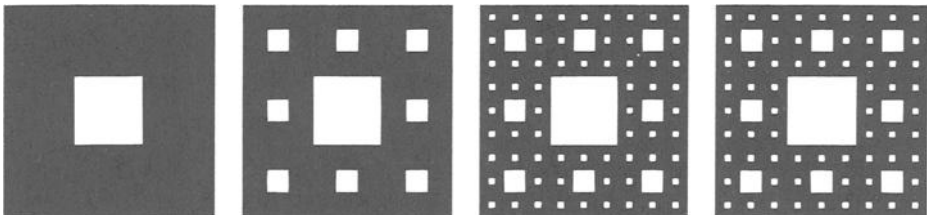

FIG. 1—*Construction of the Sierpinski "carpet". The initiator is a square and the generator is composed of N = 8 squares. They are obtained by contractions of ratio r = 1/3. Four construction stages are shown (D = ln 8/ln 3 = 1.89 . . .) [11].*

Pyrolysis followed by gas chromatographic separation of the volatile decomposition products (pyrolysis-GC) is a commonly employed analysis method in many different scientific domains including criminalistics; pyrograms generated from unknown organic substances may be compared to those produced from reference compounds under the same conditions [14]. Takatsu and Yamamoto [15,16] have studied the soot produced from the combustion of 8 aromatic hydrocarbons (benzene, toluene, o-xylene, m-xylene, p-xylene, styrene, cumene and ethylbenzene) using a Curie-point pyrolyser (at 358°C and 590°C) coupled to a gas chromatograph. The pyrograms obtained were differentiated by their characteristic content with respect to benzene, toluene, o/m/p-xylene, styrene and biphenyl. The presence of xylene and biphenyl, for example, was specific for soot produced from xylene and benzene, respectively. These characteristic compositions were found in soot samples aged up to one year. In all soot samples studied, the authors were able to identify polycyclic components such as naphthalene and anthracene, in addition to some oxygenated components (cresol and xylenol, for example). The presence of oxygenated species in the soot deposit appeared to be closely related to the chemical structure of the parent combustible.

Saltzman and Berg [17], as well as Vorhees and coworkers [18], used pyrolysis techniques to study the inorganic and organic content (particularly the SOF) characterizing atmospheric pollutants in the form of solid particles including soot.

The polycyclic aromatic hydrocarbons (PAH's), major components in the soluble organic fraction (SOF), may be defined as organic structures composed of at least two fused benzene rings which may be modified by one or many functional groups. These compounds are generally of anthropogenic origin, but may also be natural [19]. Table 1 details the PAH compounds that were detected in soot samples analyzed in this present study.

PAH's have been identified in many different media including soot and urban air [20], petroleum-derived combustibles [21], car exhaust fumes [22], and cigarette smoke [23]. The PAH's are generally present in the form of complex mixtures of various isomeric structures and alkylated derivatives, where the relative concentrations and mutagenic or carcinogenic properties vary for each component. These properties have been the subject of numerous studies [24,25].

In petroleum, PAH's are present in variable quantities; their degree of alkylation is significantly different to that observed for substances produced during the combustion process [26]. The majority of the PAH's contained in the smoke from the incineration of wood, for example, is non-substituted; the anthropogenic formation of PAH's by pyrolysis (at high temperature, organic substances partially break into smaller, unstable molecules) or by pyrosynthesis (the fragments, essentially free radicals, combine to form larger, more stable molecules) has the effect of significantly reducing the length of the alkyl chains in the PAH's contained in the parent fuel. Exhaust gases, for example, typically contain PAH's alkylated by one or two carbons.

As the PAH's are to some extent consumed during the soot formation process, only the more stable components, composed of 3 or 4 aromatic rings (more flame resistant), generally remain. According to Hirschler [27,28], these species are also very similar to those identified in the smoke produced by the combustion of various polymers (polyethylene, polypropylene, polystyrene, PVC), even though the quantities formed are often quite different. Some examples are given in Table 2.

The results suggest that 3 or 4-ringed hydrocarbons are much more stable than those composed of only 1 or 2 rings and that PAH's are formed by similar mechanisms whether from the combustion of certain polymers or simple fuels. It appears that these PAH's are stable coproducts formed in the reaction rather than simply cooled intermediates. However, several authors, including Pedersen and Ingwersen [31], believe that the aromatic content and the chemical nature of the combustible, in addition to its PAH content, have a strong influence on the quantity and type of PAH's emitted during the combustion process.

TABLE 1—*Names and structures of the principal polycyclic aromatic hydrocarbons (PAH's) considered in this study.*
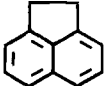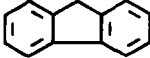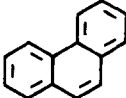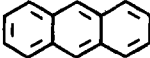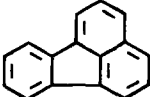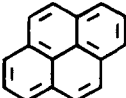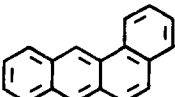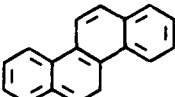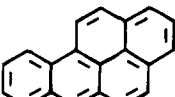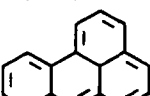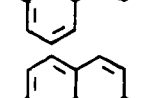
Structure	PAH	ABR.	Empirical formula	mw
	Acenaphtene	ACE	$C_{12}H_{10}$	154.21
	Fluorene	FLUO	$C_{13}H_{10}$	166.23
	Phenanthrene	PH	$C_{14}H_{10}$	178.24
	Anthracene	AN	$C_{14}H_{10}$	178.24
	Fluoranthene	Fluoran	$C_{16}H_{10}$	202.26
	Pyrene	PY	$C_{16}H_{10}$	202.26
	Benzo[a]anthracene	BaAN	$C_{18}H_{12}$	228.30
	Chrysene	Chrys	$C_{18}H_{12}$	228.30
	Benzo[a]pyrene	BaP	$C_{20}H_{12}$	252.32
	Perylene	PER	$C_{20}H_{12}$	252.32
	Benzo[ghi]perylene	BghiPER	$C_{22}H_{12}$	276.34

TABLE 2—*PAH quantities found in the soot particles formed from the combustion of three different synthetic polymers: polyethylene (PE), polypropylene (PP), and polyvinylchloride (PVC). (Sources: * = [29]; ** = [30])*

	Concentration in soot (mole %)		
PAH	PE*	PP*	PVC**
Flourene	—	0.01	0.61
Phenanthrene Anthracene	12.47	14.85	14.25
Fluoranthene	18.98	24.15	25.11
Pyrene	46.38	30.83	25.11
Benzo[a]anthracene Chrysene	8.59	5.03	9.12
Benzo[a,e]pyrene	—	5.85	1.26
Perylene	—	5.69	1.26
Benzo[ghi]perylene	—	2.08	0

Akhter and coworkers [32,33] have studied soot samples, resulting from the combustion of n-hexane, by the following techniques: infrared spectroscopy (FTIR), Raman spectroscopy, C^{13} nuclear magnetic resonance (NMR) spectroscopy, and electronic paramagnetic resonance (EPR) spectroscopy. In subsequent analyses, the soluble organic fractions from the same samples were studied by GC-MS, FTIR, UV-visible spectroscopy, fluorescence and NMR. The results showed that the solvent-extracted components were aromatic and oxygenated aromatic compounds and their alkylated derivatives. The following compounds were identified by UV spectroscopy, fluorescence and GC-MS: pyrene, perylene, picene, chrysene, fluorantene and their alkylated derivatives. The C^{13} NMR studies indicated that the ratio between aromatic and aliphatic components was at least 9 to 1. This ratio was confirmed by FTIR, Raman and EPR spectroscopy.

The purpose of this study was to verify to what extent the soots produced by the combustion of various products (mostly petroleum derivatives) could be differentiated on the basis of:

• physical parameters (such as the fractal dimension D) related to the morphology of the aggregates and elementary soot particles; and
• chemical studies, either by total chromatographic profiles ("fingerprints") obtained by GC-FID and pyrolysis-GC) or by the detection and identification (by GC-FID and GC-MS) of several chosen PAH's.

Experimental Procedure

Choice of Combustibles

Twenty liquid or semi-liquid products (L) [including two control samples: a solvent (toluene) and a solution of toluene containing four common polycyclic aromatic hydrocarbons (PAH's)], and three oils (two motor oils and one brake fluid), were chosen as combustibles. The oil samples were judged to be of interest for the investigation of vehicle fires [34].

The choice of accelerants was based on results obtained from casework at the Institut de Police Scientifique et de Criminologie (IPSC), University of Lausanne, from 1988 to 1992. Gasoline, for example, was detected in 90% of the cases where an accelerant was present. The other products, aside from the control samples, were identified in at least one case over the specified period. In addition, 12 plastic samples (P), representative of 7 common polymer classes (hydrocarbon-derived polymers where the resulting soot was to be

compared with that from typical accelerants), particularly those employed by the packaging industry, were included in the collection.

The selected liquid and plastic materials, their nature, composition and origin, are indicated in Table 3.

Soot Sampling Method

All the combustion experiments were conducted in a weakly ventilated laboratory fume hood. An air supply was guaranteed by a 15 cm opening at the front of the fume hood in addition to an open laboratory window at a distance of approximately 250 cm from the fume hood.

Samples L1 to L20 and P1 to P12 were burnt in 150 mL beakers and in crystallization dishes, respectively. The crystallization dishes were placed in aluminum tins as the heat released during the combustion of the polymers was often very intense.

The ignition of the products was achieved with the flame of a Bunsen burner applied directly to the surface of the sample, the heat source being removed once independent combustion was attained. For the combustibles which tended to extinguish themselves, the Bunsen burner was continually reapplied in order to maintain continual combustion. For the freely burning plastic samples, combustion was maintained by the continual addition of unburned material. As the physical state of a solid sample, particularly its geometry, considerably influences the quantity of soot produced [*35*], samples P1 to P12 were reduced to small pieces of roughly equivalent dimensions (maximum size approx. 2 × 3 × 5 cm) before combustion.

The simultaneous variation of numerous parameters including ventilation, ignition source, quantity of combustible, mixtures of combustibles, temperature and pressure variations, fire geometry, etc., could not be realized in this study. This is despite the fact that such factors would need to be considered if a real fire situation were to be simulated. Due to practical limitations, only two variables were considered: combustion time and combustible type.

Results obtained from a preliminary study [*36*] had shown that, for a particular fuel type, the combustion time (t_{comb}) does not have a significant influence on the evolution of different soot forms. For this reason, the duration of combustion was chosen essentially as a function of the quantity of soot necessary to conduct the proposed sequence of examinations. The chosen samples were therefore burnt over a period of 1 hour. For the liquid or semi-liquid samples (L1–L20), a quantity of 125 mL was sufficient to guarantee combustion over this period. For the solid samples, combustion over 1 hour was achieved by the continual addition of unburned material. The resulting soot was collected on glass sheets (named "0-sheets" in this study) placed on two metal rods over the opening of the smoke duct as shown in Fig. 2. After each experiment, the glass sheets were replaced and the installation cleaned thoroughly with acetone.

Five blind samples (I1 to I5) were prepared by other colleagues in the laboratory using the same combustion conditions as described for the other samples; only the combustion time was varied (35 min $\leq t_{comb} \leq$ 60 min). The identity of these "unknown" samples was revealed once the final results had been established: I1 = L5 (t_{comb} = 35 min), I2 = L20 (t_{comb} = 45 min), I3 = P8 (t_{comb} = 40 min), I4 = P9 (t_{comb} = 60 min), I5 = L2 (t_{comb} = 45 min).

In addition, 12 casework samples (window glass fragments covered in soot), taken from the scene of 8 fires in French-speaking Switzerland between 1990 and 1991, completed the collection (Samples R1 to R8, Table 4). One of the authors (Pinorini) was present at the fire scene in each case to ensure that soot samples were collected in a standardized manner.

The chosen soot removal method (Fig. 3) permitted the transfer of soot particles from the 0-sheets and the R-fragments (the casework window glass samples) onto microgratings; the technique was developed to guarantee sampling uniformity both for experimental and

TABLE 3—*Details of the reference liquid (L) and plastic (P) combustibles employed in this study for the production of corresponding soot samples. (*h.f. = hydrocarbon fraction)*

| No.	Sample	Brand or Supplier	Composition
L1	Denatured alcohol	Migros (# 5020.800)	principally ethanol mixed with MEK and MIK
L2	Paraffin oil	Migros (# 5020.805)	alkane mixture: C7 to C14
L3	White spirit	Fripoo-Produkte, Grüningen, Switzerland	h.f.* C8 to C13
L4	Leaded "super" gasoline	Shell	h.f. C5 to C12
L5	Unleaded gasoline	Shell	h.f. C5 to C12
L6	Diesel	Shell	h.f. C10 to C25
L7	Kerosene	Fluka Chemie AG, Buch, Switzerland	h.f. C9 to C15
L8	Turpentine	Droguerie Dessaux, Lausanne, Switzerland	mixture of natural terpenes and other aromatics
L9	Charcoal lighter fluid	Migros (# 7536.156)	h.f. C9 to C15
L10	Paint thinner	JDomit AG, Oberhasli, Switzerland	h.f. C4 to C10
L11	Paintbrush cleaner	Hopham AG, Näfels, Switzerland	mixture of natural terpenes and limonene esters
L12	Scale model fuel	Winoil Chemie AG, Wynau, Switzerland	80% methanol, 10% castor oil, 10% nitromethane
L13	CM paint thinner	Bally CTU, Schönenwerd, Switzerland	h.f. < C8 (particularly toluene) plus traces of simple alcohols
L14	ST paint thinner	Bally CTU, Schönenwerd, Switzerland	h.f. < C8
L15	2-stroke motor oil	Castrol (# X04W013S)	heavy hydrocarbon fraction
L16	Brake fluid	Lockheed (# 329s)	hydrocarbons and other compounds < C22; also contains monomethylether. and triethyleneglycol
L17	Toluene	Fluka Chemie AG, Buch, Switzerland	*purum*, > 99% toluene by GC
L18	Clear varnish	Jallut SA, Bussigny, Switzerland	white spirit with Pb and Co drying agents (1.8 %)
L19	Solution of PAH's in toluene		1 g of each of the following in 250 mL toluene: phenanthrene, anthracene, pyrene and fluoranthene
L20	4-stroke motor oil	BP (# 026608)	heavy hydrocarbon fraction
P1	Linoleum (gray)		polyvinylchloride (PVC)
P2	Insulation tubing		low-density polyethylene (LDPE)
P3	Plinth		polyvinylchloride (PVC)
P4	Packing material		expanded polystyrene (PS)
P5	Foam padding		polyethyleneterephthalate (PET)
P6	Foam padding		polyurethane (PU)
P7	Plastic bags		high-density polyethylene (HDPE)
P8	Plastic containers		polystyrene (PS)
P9	Plastic containers		polypropylene (PP)
P10	Carpet		PVC, polyamide, polyethylene
P11	Vinyl covering		PVC
P12	Synthetic fabric		Polyamide (nylon 66)
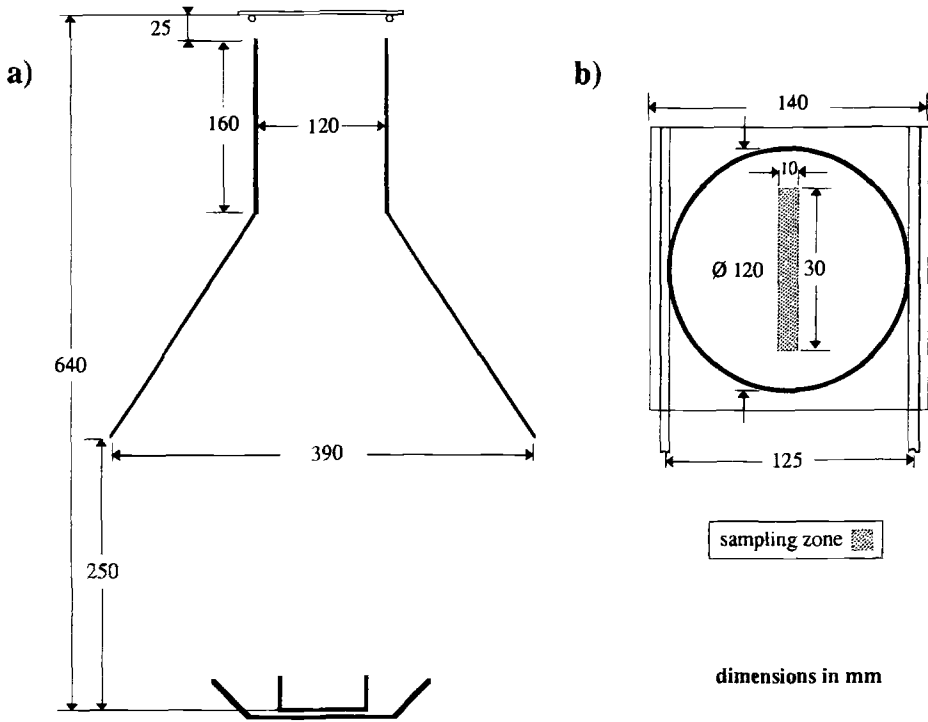
FIG. 2—*Set-up used for soot production and collection: a) side view; b) view from above, showing the position and the dimensions of the glass sheet. (The dotted region corresponds to the sampling zone for the pyrolysis-GC studies.)*

casework samples. The transfer was achieved with the aid of an electromagnetic mechanism fitted to an adjustable mechanical arm. With this system, it is possible to position the micrograting just above the soot layer (on the 0-sheet or the R-fragment), to gently release the grating onto the soot, and to then recover the grating (with the now attached soot particles). A detailed description of the soot sampling mechanism is described elsewhere [36]. All surfaces which could potentially come into contact with the soot were cleaned with acetone after each sampling experiment. In a preliminary study, it was also verified that the sampling method did not alter the morphology of the soot aggregates [36].

TABLE 4—*Details of the casework soot samples analyzed in this study.*

Samples	Date of fire	Information
R1	Oct. 6, 1990	commercial establishment (garage); various hydrocarbons detected by GC
R2	Mar. 25, 1991	residence (apartment); no accelerant detected
R3	Apr. 3, 1991	residence (farm); no accelerant detected
R4	Oct. 11, 1990	commercial establishment (distillery); benzene and toluene detected (probably from the pyrolysis of plastic materials at the scene)
R5A, B & C	Apr. 10, 1991	residence (apartment); no accelerant detected
R6A & B	Aug. 6, 1990	industrial complex (storage of carpet); no accelerant detected
R7A & B	May 20, 1990	residence; methylated spirits and gasoline used to start the fire
R8	Jan. 16, 1990	residence (chalet); gasoline and diesel present
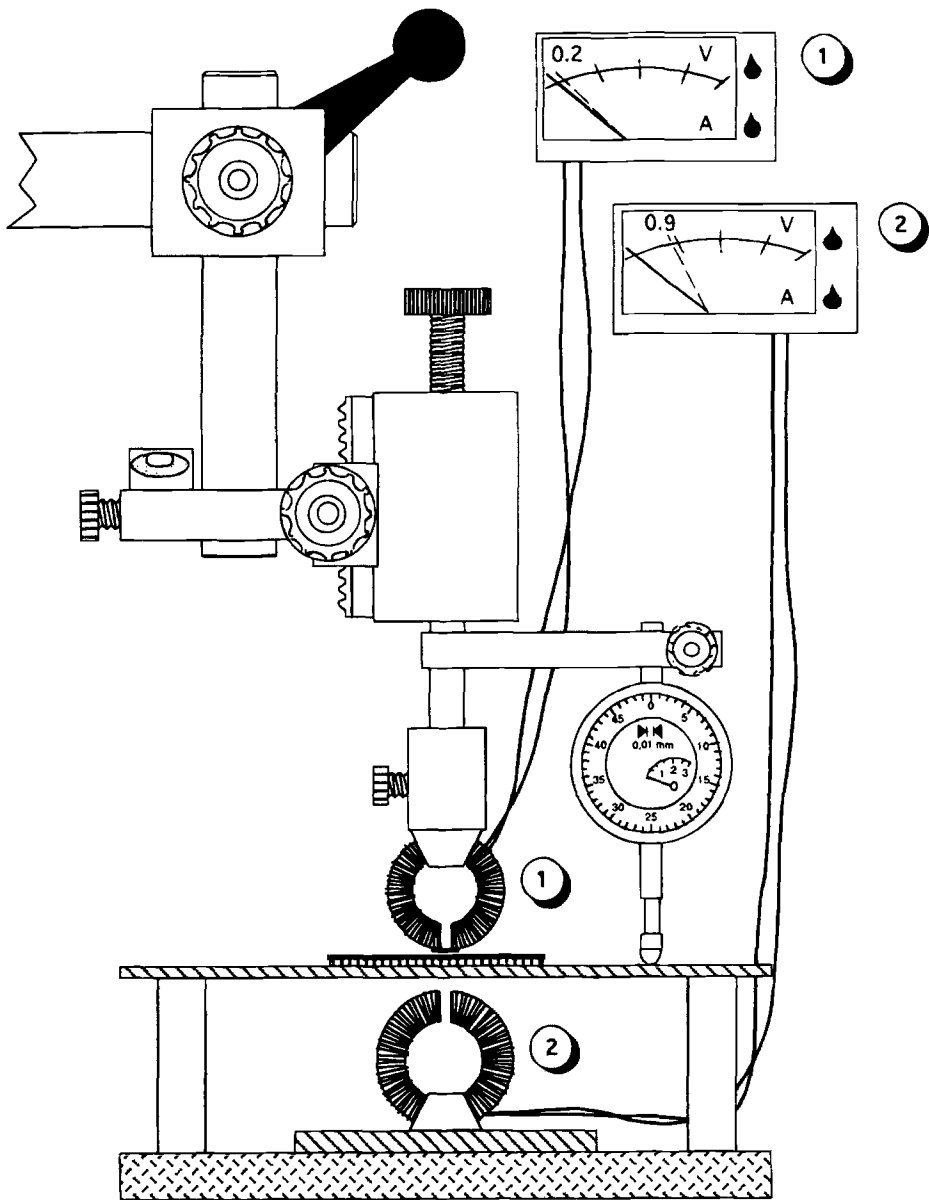
FIG. 3—*Device used for the transfer of soot particles from the glass sheets (and casework glass fragments) onto TEM micrographs. The system is based on two electromagnetics, one being used to release and then recover the micrograting (electromagnet #1) and the second being employed to ensure sufficient contact between the micrograting and the soot layer (electromagnet #2). Full details of this apparatus may be found elsewhere* [36].

For the soot recovery technique, 3 mm diameter nickel micrographs were employed (Balzers Union AG, Balzers). Before use, these were coated with a Formvar membrane (0.3% solution in dichloroethane) on which was evaporated a thin layer of carbon (1–2 nm) using a Balzers 370 coating unit.

The soot samples, collected by the described procedure, were subjected to a sequence of physical and chemical analyses as illustrated in Figure 4.

Macroscopic and Microscopic Analyses

The soot samples on the 0-sheets and the R-fragments were observed and photographed using a macroscope (low-power stereo microscope) with a magnification up to 35 ×. As the soot found at the center of the glass sheets is sometimes very different from that found at the edges (essentially due to the particular geometry of the experimental set-up), several images were recorded in these two zones. The resulting macrographs were visually compared.

Macroscopic observations were performed on a Wild M 420 macroscope (Wild/Leitz, Heerbrugg) fitted with an Apozoom objective 5.8× − 35×. Exposure times for the macrographs were automatically calculated using a Wild MP 46 processor linked to the macroscope. Images were recorded on Kodak TP-120 film (at 64 ASA) which was developed with Kodak D-19 developer.

The soot samples on the micrographs were then observed using a Hitachi HU-12 transmission electron microscope (Hitachi Ltd., Tokyo) operating at 75 kV. Before observation, the micrographs were coated with a thin layer of carbon (Balzers 370 coating unit) in order to stabilize the soot particles. In a preliminary study [36], it was verified that this
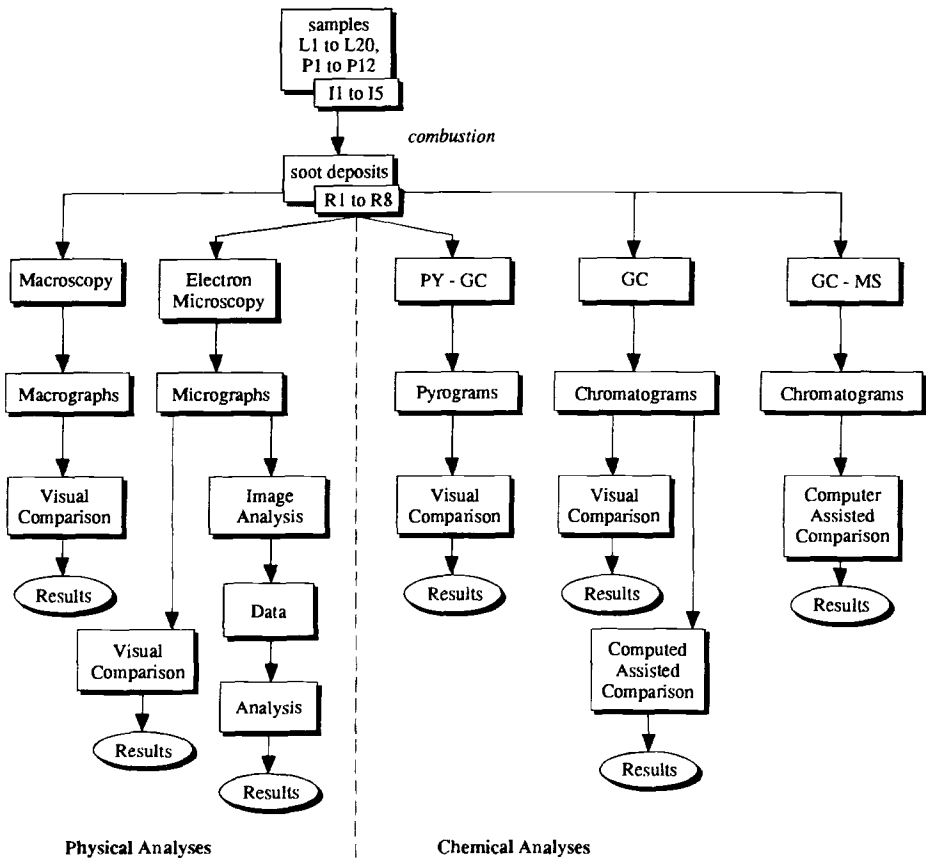

FIG. 4—*The sequence of physical and chemical analyses applied to the study of soot deposits.*

protective layer did not influence the morphology of the soot particles (ie. comparisons were done with and without the protective layer).

TEM micrographs were recorded on Kodak SO-163 negatives, developed in Kodak D-19 developer. At least three images were recorded per micrograting, taken at predetermined points that were maintained for all observations. These images were in turn digitized using an Eikonix high-resolution CCD camera. Image analysis was performed using commercially available software ("Semper 6", Synoptics Ltd., England).

The following terms were employed for the description of the various soot forms observed: "elementary particles" (e.p.; quasi-spherical base units), "typical aggregates" (aggregates formed from more or less fusioned elementary particles), "primary forms" (structures composed of small centers and typical aggregates), "characteristic soot" (soot showing specific classification elements), and "rich soot" (soot formed by combustibles producing large amounts of smoke—the soluble organic fraction characterizing this type of soot is particularly rich). In addition, the soot aggregates were classified as type 1 (typical aggregates), 2 (aggregates with some crushed portions) or 3 (significantly degraded aggregates).

The image analysis of the soot aggregates was based on the determination of four principal parameters: the perimeter (P), the surface area (S), and the two principal surface moments (M1 and M2). These values were used to calculate two supplementary parameters: the circularity (C) and the ratio of the surface moments (M1/M2). The six parameters were among the values supplied by the image analysis software employed and are defined in Table 5.

The form of a particle may only be defined when the two parameters circularity (C) and ratio of moments (M1/M2) are considered simultaneously. The notion of circularity on its own is not sufficient as, on several occasions (for example, in the case of particles with edges that are particularly jagged), the information is artificially perturbed. This remark is illustrated by Fig. 5.

The data obtained for the six parameters (P, S, M1, M2, C, M1/M2) were the subject of a discriminant analysis [37] performed with the aid of a SPSS program [38]. Eight variables in total were considered:

Y (1,2,3,4)   = average (X1, X2, X3, X4)   [principal variables]

Z (1,2,3,4)   = standard deviation (X1, X2, X3, X4)   [secondary variables]

where

$$X1 = \ln(S)$$
$$X2 = \ln\left(\frac{c}{1-c}\right)$$
$$X3 = \ln\left[\frac{M1/M2}{1-(M1/M2)}\right]$$
$$X4 = \ln(M1)$$
$$S = \text{surface of soot aggregate}$$
$$C = \text{circularity of soot aggregate}$$
$$M1 = \text{minimal surface moment}$$
$$M2 = \text{maximum surface moment}$$
$$M1/M2 = \text{ratio of principal surface moments}$$

The variables X1 and X2, X3, X4 contain the information on the size and the form of

TABLE 5—*Definitions of the parameters considered for the image analysis of selected soot particles.*

Parameter	Definition	Information
Perimeter (nm)	P = length of the line delimiting the particle	size
Surface area (nm^2)	S = surface of the particle or aggregate	size
Circularity	$C = 4pS/(P^2)$ varies between 0 and 1 (a circle gives $C = 1$)	form
Principal moments (nm^2)	Surface moments with respect to a pair of perpendicular axes (where the point of intersection is the center of the particle) in the direction of the moments min (M1) and max (M2)	form
Ratio of principal moments	M1/M2 varies between 0 and 1	form

the soot aggregate under consideration. It is for the needs of the discriminant analysis that the original variables have undergone the simple mathematical transformations indicated.

A seventh parameter (independent) is used to characterize the structure of the soot aggregates: the "fractal dimension." The considerations which follow are only valid if soot is conceived as an aggregation of *quasi-spherical* elementary particles (base units), something that is commonly accepted in this domain [*39*].

Recent measurements of the fractal dimension of an aggregate, given by the equation:

$$N = \rho \left(\frac{R}{R_0}\right)^D \qquad N \rightarrow \infty \tag{1}$$

where

R_0 = the smallest radius measured for a particle (smallest characteristic length scale)
R = radius of a circular region under consideration
N = number of constitutive units
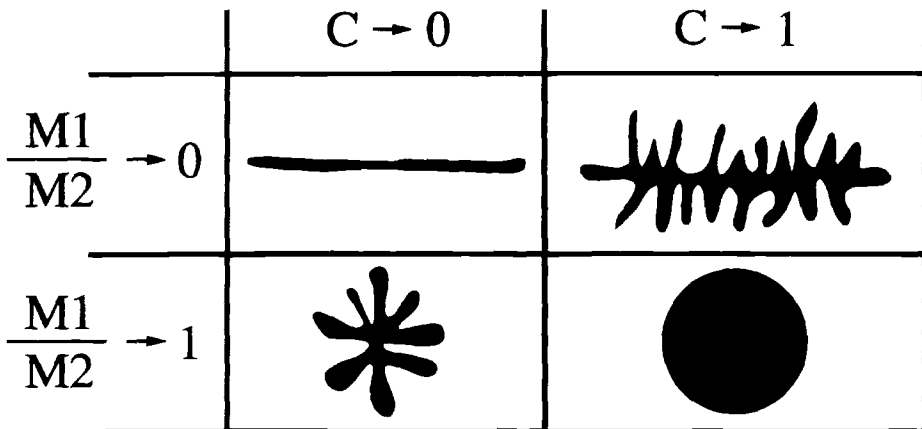ρ = surface density, which depends on how the base units are disposed (compacted)

FIG. 5—*Graphical representation of the calculated parameters C and $M1/M2$.*

have been published for different systems and it has been shown that the description of experimental results in terms of fractals is particularly useful, leading to a rationalization of the findings [11]. In this number-radius relation, D is a quantitative measure of the way in which the aggregate fills the space which it occupies; in other words, it is the aggregation mode of the constitutive units.

From equation (1), assuming that the elementary particles have an identical mass, then

$$
\begin{aligned}
N &= \text{number of spheres (or elementary particles)} \\
R &= \text{size (aggregate surface area)} \\
\ln(N) &= \ln(\rho) + D[\ln(R) - \ln(R_0)] \\
&= \ln(\rho) - D \ln(R_0) + D \ln(R)
\end{aligned}
\tag{2}
$$

where the term "$\ln(\rho) - D \ln(R_0)$" is a constant.

Given that the form and the arrangement of the constitutive units which affect ρ are not determining factors for the value of D, we can consider that:

$$N = \text{number of spheres}$$

$$= \frac{\text{total surfaces area}}{\text{surface of one sphere}}$$

$$R = \frac{\text{diameter of smallest circle containing the aggregate}}{\text{diameter of one sphere}}$$

The graphical representation of $\ln(N) = f[\ln(R)]$ is a straight line where the gradient corresponds to the fractal dimension D of the aggregate [see equation (2)].

Unlike ideal fractal objects, natural fractal objects do not generally have an identical structure at all magnifications (that is, at all length scales). In practice, there is a limiting size range outside of which the natural object is no longer fractal [40]. In our case, the lower limit is represented by a pixel in the micrographs and the upper limit by the size of the soot aggregate. With this in mind, it is not surprising that outside these limits, deviations occur by comparison with the linear function given by $\ln(N) = f[\ln(R)]$.

In practice, the fractal analysis is performed on binary images (Fig. 6). The image is successively masked with 15 concentric circles of increasing diameter: the diameter of the 15th circle (the last) corresponding to the smallest circle enclosing the aggregate. For each mask, the $\ln(N)$ and $\ln(R)$ values are calculated. The fractal dimension of an aggregate corresponds to the gradient of the linear regression resulting from the plot of the 15 $\ln(N)$ values against the 15 $\ln(R)$ values. The average fractal dimension D is calculated for each sample. The validity of the program was verified by the analysis of images of gold aggregates (Fig. 7); the results were compared with the values published by Weitz and Huang [41].

Chemical Analyses

The chemical composition of each soot sample was studied with the aid of the following chromatographic techniques: gas chromatography (GC) with and without pyrolysis of the sample, with detection by flame ionization (FID) or mass spectrometry (MS). Given the major role that PAH's play in the formation of soot and as principal components of the SOF, particular emphasis was placed on their study. In a preliminary evaluation [36], it was determined that common PAH's, especially those composed of three aromatic rings, were present in most of the soots obtained from the combustion of hydrocarbon-based liquids.

The following chemical studies were performed on the reference soot samples [obtained from the combustion of liquid (L) and plastic (P) materials], on control soot deposits prepared by a colleague (I), and on several casework samples (R):
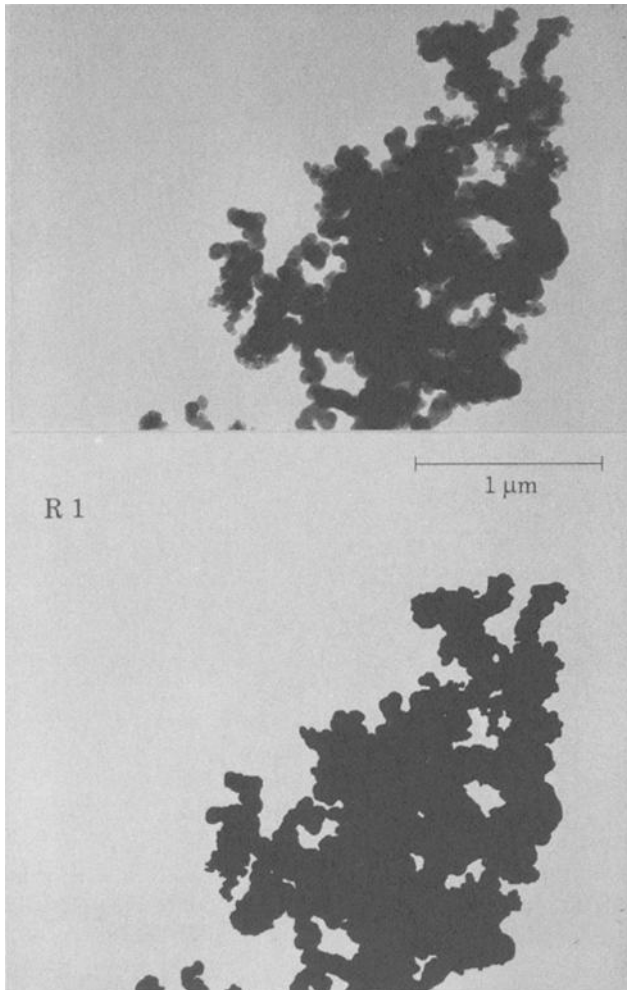
FIG. 6—*Transmission electron micrograph* (above) *of a soot aggregate from sample R1 and its corresponding binary image* (below).

    i) chromatograms recorded by GC-FID and pyrolysis-GC were compared visually (GC-vis) and automatically (GC-auto) by means of a user-generated computer program;

    ii) qualitative analysis of specific PAH markers by GC-FID (by comparison with standard reference compounds) and by GC-MS (identification based on mass spectra of individual peaks);

    iii) semi-quantitative analysis of specific PAH markers by GC-FID using an internal standard (tetradecane).

Pyrolysis-Gas Chromatography

    From the 0-sheets (the glass sheets on which the laboratory soot samples were originally deposited) and the glass fragments from real cases (R-fragments), a sample of soot (from 50 to 100 μg, depending on the type of soot) was removed by scraping with a fine metal wire. The soot samples were taken from the central region of each glass sheet (Fig. 2b).

FIG. 7—*Binary images from transmission electron micrographs of gold clusters of different sizes* [11,41].

This region was more exposed to the flames than the soot towards the edge of the deposit. The SOF characterizing this central region would therefore be expected to be less rich than the lesser exposed 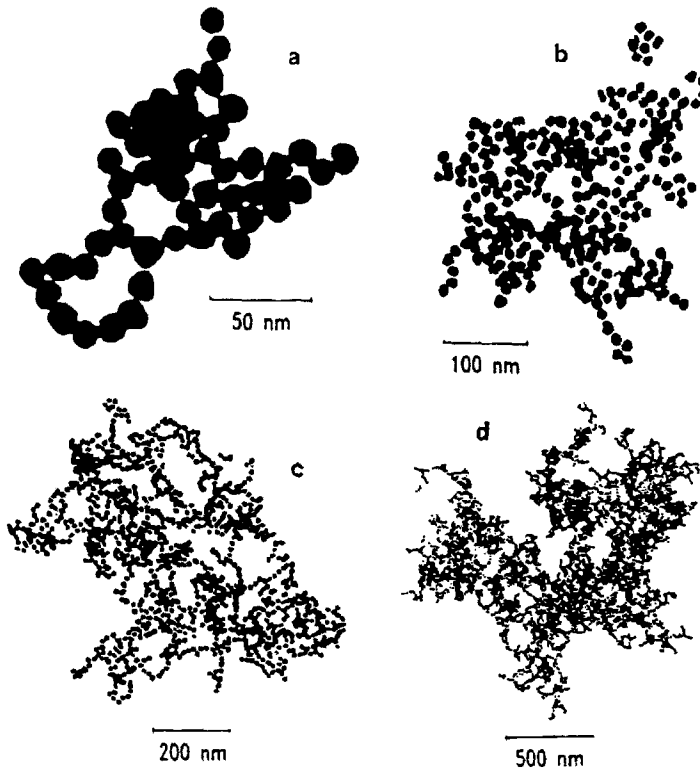soot. This sample was then deposited in the center of a 30 × 5 mm quartz pyrolysis tube which was subsequently inserted into the cylindrical filament of the pyrolysis probe (CDS Instruments, Oxford, Pennsylvania). A drop of acetone was used to block the end of the quartz tube so that the gas flow from the gas chromatograph, during insertion of the pyrolysis probe into the injector, did not dislodge the soot.

The pyrolysis was performed using a CDS 190 Pyroprobe (CDS Instruments, Oxford, Pennsylvania) operating at 600°C for a period of 20 seconds. Pyrolysis products were separated on a Perkin Elmer 8500 gas chromatograph (Perkin Elmer Ltd.) fitted with a 30 m capillary column (0.32 mm internal diameter, DB-5 stationary phase, 1.0 μm film thickness; J & W Scientific) and operating under the following parameters: 50°C initial temperature, held for 3 min, ramp rate 5°C/min up to 280°C, held for 20 min (total analysis time = 69 min; injector 260°C, FID 320°C, carrier gas [He] flow rate 2 mL/min). The resulting pyrograms were recorded on a Perkin Elmer GP-110 Graphics Printer.

Several soot samples could not be analyzed by pyrolysis-GC, either because of insufficient quantity (L1, L2, L12, I5), or because the sample, due to its condition, could not be adequately scraped off the glass support (L9, L11, L16, I1, R2).

Gas Chromatography (GC-FID and GC-MS)

The soot remaining on the 0-sheets and the R-fragments after the preceding treatment was collected by rubbing with cotton gauze soaked in diethyl ether. The increase in weight

of the cotton gauze, after evaporation of the solvent, was used to calculate the quantity of soot recovered from each sample (Table 6).

The SOF of each sample was isolated by Soxhlet extraction of the cotton gauze with cyclohexane (200 mL) over 3 hours. Tetradecane was added as an internal standard. The extract was evaporated down to approximately 5 mL using a rotary evaporator ("Rotavapor"; Büchi) then filtered. The filtrate was concentrated under a flow of nitrogen down to a final volume of between 0.6 and 0.8 mL. Background (blank) samples were similarly prepared by the extraction of cotton gauze without soot. The resulting concentrated samples were stored at 4°C before chromatographic analysis. (This extraction procedure was verified in a preliminary study [36]. In quantitative terms, the process extracts approximately 85% of available PAH's. The extraction was also shown to be non-selective; linear calibration curves were recorded for all PAH's tested.)

The extracts were analyzed using a Carlo Erba HRGC 5300 gas chromatograph (Carlo Erba Strumentazione) using a split/splitless injector in the split mode (split ratio: 50:1) and under the same chromatographic conditions as described above (pyrolysis-GC). For each sample, two separate injections of 5 μL were employed. The resulting chromatograms were recorded and integrated on a SIC Chromatocorder 12 processor (System Instruments Co., Ltd.)

Chromatograms were compared visually and with the aid of a user-generated computer program [written by one of the authors (Lennard) on an Apple Macintosh computer using Microsoft Basic programming software]. The computer program permitted the comparison of chromatograms based on the normalized peak surface areas of 103 selected compounds [calculated by reference to the internal standard peak (tetradecane) in each case]. Different comparison algorithms were assessed, with the following system being finally accepted as

TABLE 6—*Quantity of soot sampled on the glass sheets (and on the casework glass fragments) and employed for the chemical analyses described.*

Sample	Quantity of soot (mg)	Sample	Quantity of soot (mg)
L1	<1	P6	17.4
L2	<1	P7	4.8
L3	15.0	P8	23.4
L4	12.0	P9	29.1
L5	10.2	P10	5.6
L6	7.7	P11	16.1
L7	10.4	P12	5.3
L8	21.7	I1	2.5
L9	2.9	I2	4.2
L10	10.4	I3	15.9
L11	4.4	I4	30.6
L12	<1	I5	<1
L13	18.9	R1	5.5
L14	3.2	R2	32.3
L15	5.1	R3	14.8
L16	2.6	R4	46.9
L17	29.2	R5A	28.6
L18	7.3	R5B	11.8
L19	23.4	R5C	20.2
L20	4.7	R6A	48.4
P1	22.0	R6B	9.9
P2	14.1	R7A	5.2
P3	8.0	R7B	5.8
P4	17.7	R8	33.1
P5	10.2		

the best for our purposes. For each chromatogram, the normalized surface areas for the 15 most intense peaks (out of the 103 target compounds) were recorded and placed in order of decreasing size.

For the comparison of two chromatograms, an initial match value (MV) of 100 was arbitrarily assigned (that is, a perfect match, where the same 15 compounds are present in the same order for both samples, gives a match value of 100). In the case where a compound is missing from the top 15, 10 points are deducted from the MV. When a peak is present but not in the correct order of intensity, the absolute value of the difference in positions, up to a maximum of 10 points, is subtracted. (For example, if a certain compound is classified in position 12 in order of decreasing intensity, but is found in position 4, then 8 points are deducted from the MV.) Various tests, including the repeated analysis of the same sample, indicated that a differentiation threshold value of 70 was acceptable (ie. non-differentiation: MV $\geq$ 70; differentiation: MV < 70).

With respect to the search for potential "markers" for soot identification, the results obtained by GC-FID were confirmed by GC-MS. These latter analyses were performed on a Hewlett Packard HP 5890 gas chromatograph connected to a Hewlett Packard HP 5971A mass selective detector (Hewlett-Packard, Avondale, PA). The GC was fitted with a 30 m DB-5 capillary column (0.25 mm internal diameter, 1.0 μm film thickness; J & W Scientific). The corresponding temperature program was identical to that presented above (pyrolysis-GC). [Injector temperature 250°C, interface (GC-MS) temperature 280°C, carrier gas [He] flow rate 2 mL/min, MS scan from 10 to 450 m/z.] Data analyses were performed on a Hewlett-Packard Vectra Q2/20 personal computer using MS Chemstation Software, version G1034B (Hewlett-Packard, Avondale, PA). Peaks due to polycyclic aromatic hydrocarbons were identified by comparison of their mass spectra to those contained in commercially available and user-generated MS libraries. Quantification of these peaks was achieved on the basis of normalized surface areas and standard curves established during a preliminary study [36].

Results

Macroscopic and Microscopic Analyses

Visual Comparison of Macrographs—The *macroscopic examination* of the soot samples permitted an evaluation of the general aspect of the deposit in addition to the detection of unburned polymer fragments, characteristic of the combustion of plastic materials.

Most of the reference soot samples (L and P) from the combustion of average to strong smoke producers could be differentiated on the basis of morphological characteristics. For samples L1, L2, L7, L12 and L16, the quantity of soot deposited was very small and the resulting macrographs could not be differentiated. The plastic deposits (Fig. 8) were easier to identify due to a more characteristic aspect compared to the soot from liquid products (Fig. 9).

The "unknown" laboratory-prepared samples I2 to I5 could all be correctly classified from macroscopic observations (Table 7). Sample I1, however, was incorrectly identified due to a weak soot deposit compared to that of the corresponding reference sample (L5). This could be explained by the reduced combustion time employed for the preparation of soot sample I1 (35 min, compared to 60 min for the reference samples).

Macroscopic examination of the casework samples (R-fragments) indicated, in most cases, the presence of thin, contaminated soot deposits that had a "washed," shiny appearance. The soot structures had a squashed appearance, with no obvious three-dimensional forms being visible (Fig. 10). A valid comparison of these degraded structures with those observed in laboratory-prepared soot samples was not possible. Most of the casework samples had been recovered from the ground or from piles of debris at fire scenes. This fact, together with
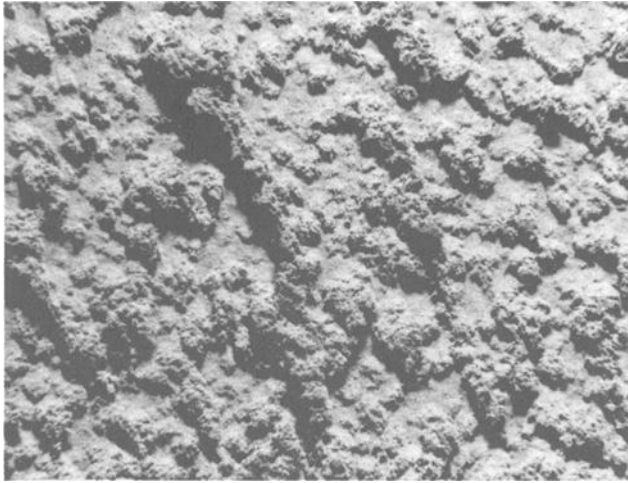
FIG. 8—*Macroscopic observation (12.5 X) of the soot deposit formed from the combustion of PVC (P11).*

the effects from various other parameters (such as water damage due to fire-fighting procedures), may explain the degraded nature and contamination of the casework soot deposits.

Visual Comparison of Micrographs

The information obtained by *microscopic examination* of the soot deposits appeared more reliable than that obtained by simple macroscopy as more intimate elements (such as the structure and morphology of individual soot aggregates), which are practically independent of the quantity of soot deposited during the fire, were observed.
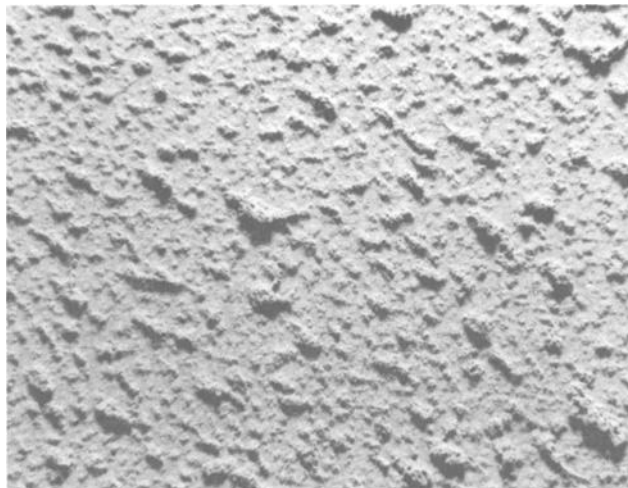

FIG. 9—*Macroscopic observation (12.5 X) of the soot deposit formed from the combustion of diesel (L6).*

TABLE 7—*Classification results obtained for the control (I) and casework (R) samples for each physical technique employed.*

Sample	Macroscopic observations	Microscopic observations	Discriminant analysis	Fractal dimension	Identity
I1	L2, L9, L11	L2, L5, L7, L9, L11, L14 L15, L18, L20, P7, P10,	P (plastic)	L2, L5, L7, L9, L11, L15, L20, P6	L5
I2	L7, L14, L15, L20	L2, L5, L7, L9, L11, L14, L15, L18, L20, P7, P10	P	L2, L5, L7, L9, L11, L15, L20, P6	L20
I3	L8, L17, L19, P4, P8	P3, P4, P6, P8, P9	L (liquid)	L3, L4, L6, L8, L10, L13, L17, L19, P1, P3, P4, P5, P7, P8, P9, P10, P11, P12	P8
I4	L4, L5, L10, P1, P9, P11	P3, P4, P6, P8, P9	P	L3, L4, L6, L8, L10, L13, L17, L19, P1, P3, P4, P5, P7, P8, P9, P10, P11, P12	P9
I5	L2, L9, L11	L2, L5, L7, L9, L11, L14, L15, L18, L20, P7, P10	P	L2, L5, L7, L9, L11, L15, L20, P6	L2
R1	?	?	?	L14, P2	?
R2	?	?	?	L14, P2	?
R3	?	?	?	L14, P2	?
R4	?	?	?	L2, L5, L7, L9, L11, L15, L20, P6	?
R5A	?	?	?	L3, L4, L6, L8, L10, L13, L17, L18, L19, P1, P3, P4, P5, P7, P8, P9, P10, P11, P12	?
R5B	?	?	?	L14, P2	?
R5C	?	?	?	P2, P7, L3, L5, L6, L14, L18, P10, P1, P11	?
R6A	?	?	?	L14, P2	?
R6B	?	?	?	L14, P2	?
R7A	?	?	?	L3, L4, L6, L8, L10, L13, L17, L18, L19, P1, P3, P4, P5, P7, P8, P9, P10, P11, P12	?
R7B	?	?	?	L3, L4, L6, L8, L10, L13, L17, L18, L19, P1, P3, P4, P5, P7, P8, P9, P10, P11, P12	?
R8	?	?	?	L2, L5, L7, L9, L11, L15, L20, P6	?

Transmission electron microscopy permitted the detection of various classification elements—polymer fragments (Fig. 11) and characteristic soot forms—and morphologically distinct soot structures. From this information, five reference samples could be unequivocally differentiated (L3, L4, P1, P2 and P11), while the remaining samples could be separated into six distinct groups (Fig. 12). The "unknown" I samples were correctly classified in each case but with greater precision for the plastic-related samples I3 and I4 (Table 7).

Particular soot forms were considered as characteristic when they were only found in soot samples from a limited range of combustibles (preferably only one) and when they were routinely observed in these cases, independent of the combustion duration. The origin
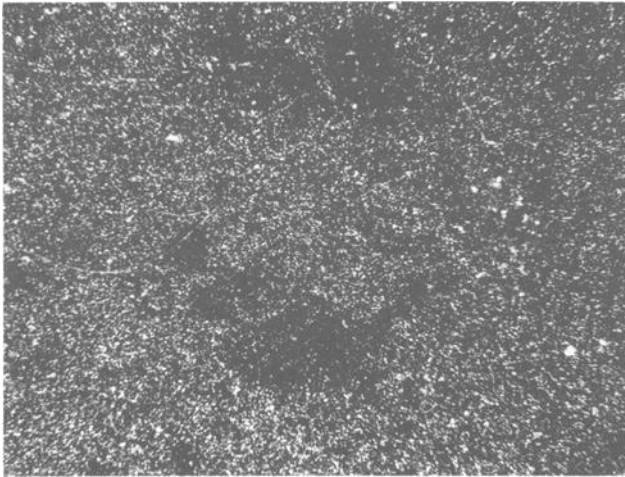
FIG. 10—*Macroscopic observation (12.5 X) of the soot deposit on the casework glass fragment R6B.*

of these characteristic forms [for example, P2, P11: "opaque spherical particles, linked by a type of amalgam" (Fig. 13); P5, P12: "veiled structures in the form of small boats" (Fig. 14)] is unknown, but their presence is probably linked to the chemical composition of the combustible.

The plastic-based soot samples were characterized by a mixture of typical soot forms, large particles (soot aggregates and polymer fragments) and various degraded structures randomly distributed over the microgratings. This can be directly related to the observed combustion of the plastic materials studied (the combustion was often lively, sometimes violent, and in all cases irregular, with large particles—soot agglomerates and polymer

FIG. 11—*Electron micrograph (5000 X) of a polymer fragment observed in soot deposit P11 (PVC).*

polymer fragments? → Y → plastic combustible

N

opaque e.p., rounded and linked? → Y → e.p. "amalgamated"? → Y → P11

→ N → P2

N

e.p. "amalgamated"? → Y → P1

N

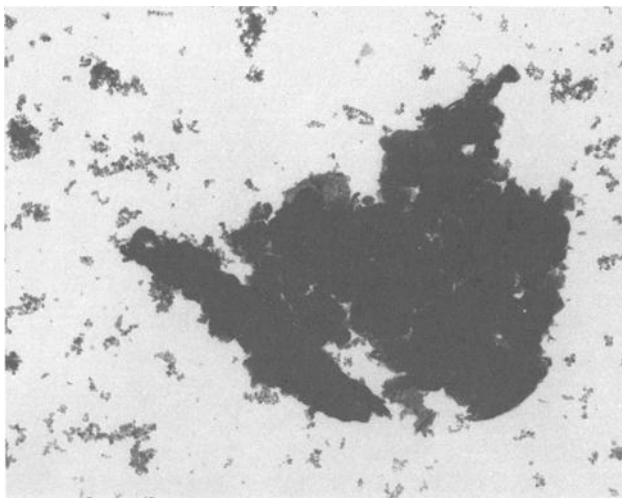veiled structures in the form of small boats? → Y → P5, P12

N

fused structures? → Y → "droplets"? → Y → L → L6, L8, L13, L17, L19

→ P → P3, P4, P6, P8, P9

→ N → L4

N

"droplets"? → Y → L3

N

ratio DA/TA > 1 → Y → L1, L12, L16

N → L → L2, L5, L7, L9, L11, L14, L15, L18, L20

→ P → P7, P10

LEGEND

e.p. = elementary particles
DA = number of degraded aggegates
TA = number of typical aggregates

▭ = differentiated samples

⬭ = non-differentiated samples

FIG. 12—*Dichotomic classification system established from the results obtained by transmission electron microscopy for the L and P reference samples.*

fragments clearly visible to the naked eye—being continually liberated). The liquid-based soot deposits, on the other hand, tended to be much more homogeneous.

All the soot aggregates located in the casework samples had, at least to some degree, a squashed appearance (Fig. 15). This phenomenon was less pronounced for samples R1, R7A and R7B, which, unlike the other R samples, had not been subject to water treatment

FIG. 13—*A characteristic soot form observed in sample P2 (LDPE) showing opaque elementary particles that are spherical and linked together (20000 X).*

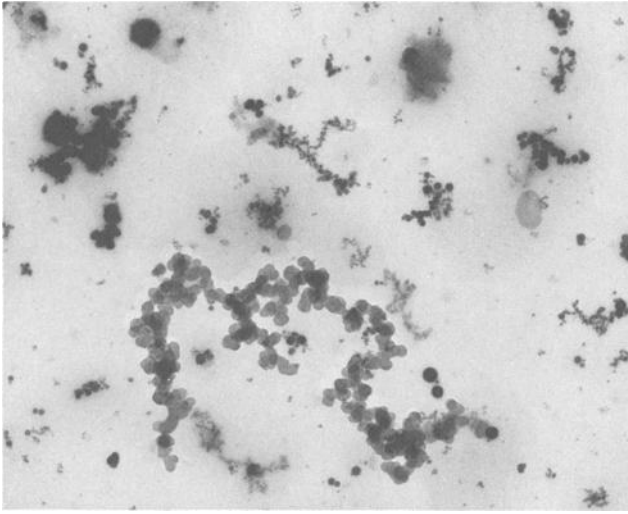during the fire-fighting procedure. In these favorable cases, the observed aggregates were similar to some of the typical soot forms characterizing the laboratory-prepared samples. Nevertheless, due to the degraded nature of the casework soot deposits, unequivoqual classifications based on microscopic observations were not possible.

Samples L1, L12 and L16 were disregarded for the remainder of the study due to the insufficient number of aggregates observed in these cases.

The descriptive features used for the classification of the soot samples from the corresponding micrographs were reproducible in the sense that, for the same sample, these
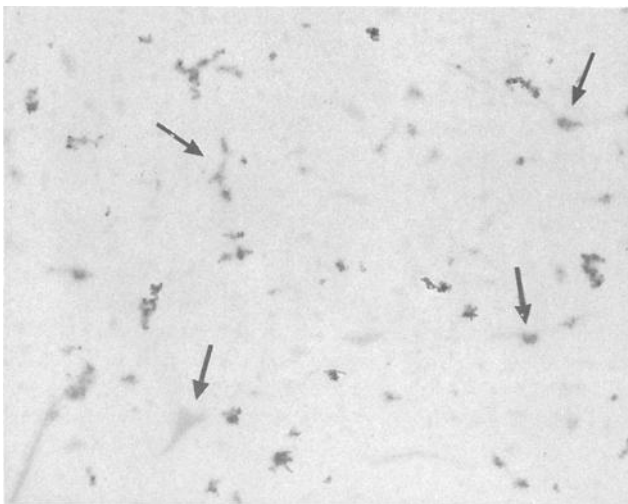

FIG. 14—*Electron micrograph (5000 X) showing veiled structures in the form of small boats (soot sample P12; polyamide).*
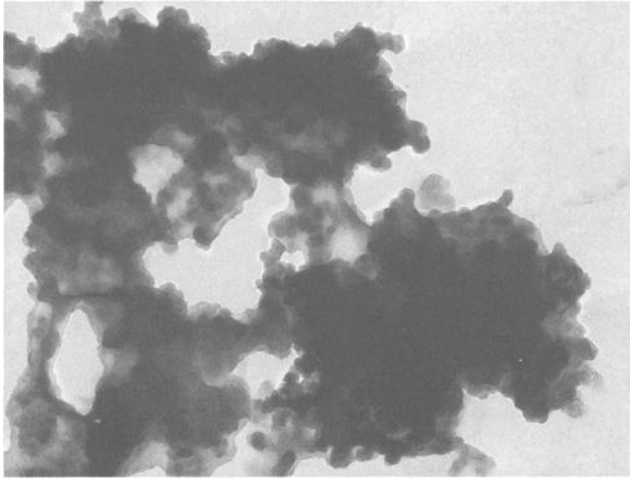
FIG. 15—*Electron micrograph (20000 X) of a "squashed" soot aggregate observed in case-work sample R2. The constitutive units are indistinct and are linked by a type of amalgam.*

features were always present (independent of the combustion time, according to a preliminary study [36]). In addition, the descriptive features were specific for certain soot types. With regard to the subjective aspect of these observations, it is clear that the ability to identify such features will depend on the experience of the person involved. In this study, one of the authors (Pinorini) spent nearly 12 months studying electron micrographs of soot deposits.

Discriminant Analysis

The discriminant analysis (Fig. 16), performed on the basis of the 8 variables associated to the size and the form of the aggregates, permitted the differentiation of most of the liquid-related soots from those resulting from the combustion of plastic materials. However, despite certain tendancies, the samples belonging to the same group (L or P) could not be unequivocally differentiated. In addition, the control samples I1 to I5 were incorrectly classified (Table 7). The behavior of the R (casework) samples was atypical in that their positions in Fig. 16 form a cloud that is significantly separated from the clouds formed by the L and P samples. This result confirmed the observation that the morphology of the R aggregates is significantly different (due to degradation) from that of the characteristic aggregates observed in the laboratory-prepared samples.

Fractal Dimension

The recorded values [average fractal dimension (D) and standard deviation (SD)] for each soot sample are given in Table 8. The typical soot aggregates (type 1), observed for the laboratory-prepared samples, were characterized by intermediate fractal dimensions situated between 1.7 and 1.9. These values are in agreement with those reported by various authors including Colbeck [9], but do not significantly vary from one sample to another. Taking into account the standard deviation for each average value of D, the aggregates of the laboratory-prepared soot samples (L, P and I) cannot be differentiated. On the other hand, if the "raw" values are considered (that is, without consideration of the standard deviations), it is possible to note certain tendencies: the rich soot aggregates (L3, L4, L6, L8, L10, L13, L17, L18, L19, P1, P3, P4, P5, P7, P8, P9) are characterized by average D
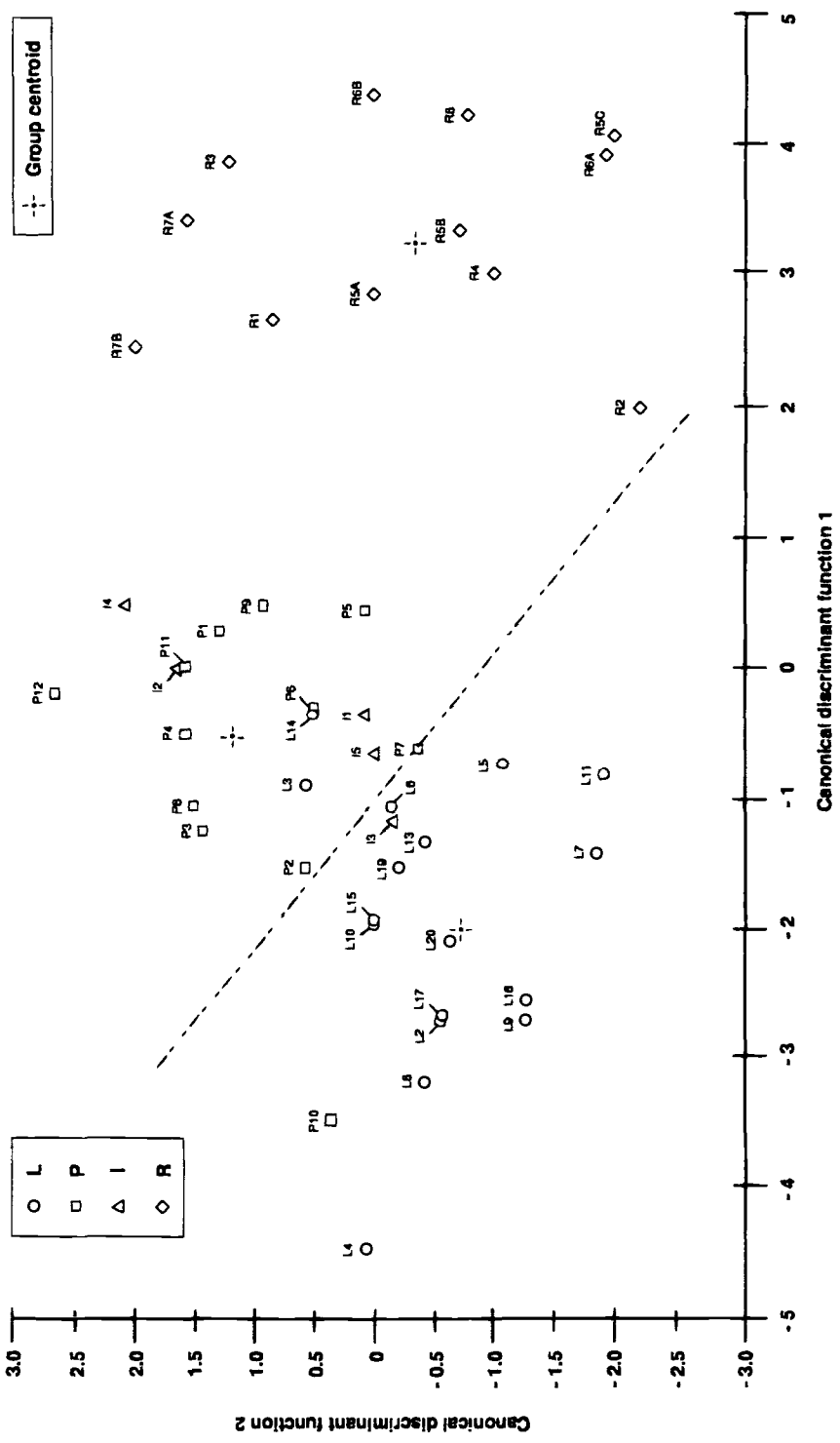
FIG. 16—*Graphical representation of the discriminant analysis showing the relative positions of the "grouped" L, P and R samples and the "ungrouped" I samples.*

TABLE 8—*Fractal dimensions calculated for all of the analyzed soot samples (D = fractal dimension; SD = standard deviation).*

Sample	D	SD	Soot form[a]
L2	1.76	0.21	1
L3	1.74	0.13	1
L4	1.73	0.07	1
L5	1.76	0.20	1
L6	1.75	0.13	1
L7	1.76	0.06	1
L8	1.73	0.38	1
L9	1.76	0.20	1
L10	1.72	0.05	1
L11	1.76	0.08	1
L13	1.74	0.12	1
L14	1.85	0.15	1
L15	1.78	0.03	1
L17	1.72	0.12	1
L18	1.75	0.10	1
L19	1.70	0.03	1
L20	1.75	0.08	1
P1	1.73	0.11	1
P2	1.85	0.32	1
P3	1.70	0.18	1
P4	1.71	0.20	1
P5	1.73	0.27	1
P6	1.80	0.07	1
P7	1.80	0.08	1
P8	1.71	0.22	1
P9	1.72	0.06	1
P10	1.74	0.12	1
P11	1.74	0.08	1
P12	1.77	0.09	1
I1	1.76	0.06	1
I2	1.76	0.04	1
I3	1.71	0.13	1
I4	1.72	0.19	1
I5	1.79	0.10	1
R1	1.81	0.06	2
R2	1.86	0.11	2
	2.40	0.07	3
R3	1.82	0.02	2
	1.94	0.15	3
R4	1.79	0.09	2
	2.20	0.09	3
R5A	1.66	0.06	2
	1.89	0.04	3
R5B	1.82	0.01	2
	2.10	0.07	3
R5C	2.30	0.06	3
R6A	1.85	0.04	2
R6B	1.83	0.02	2
R7A	1.74	0.14	2
R7B	1.72	0.04	2
R8	1.76	0.04	2
	1.93	0.06	3

[a]Soot form: 1 = typical aggregates; 2 = typical aggregates where the elementary particles are partially squashed and/or fused; 3 = various degraded structures.

values varying from 1.70 to 1.75, while, for samples from weak soot producers (such as L2, L5, L7, L9, L11, L15, L20), the variation is from 1.75 to 1.80. For samples L14 and P2, D lies between 1.80 and 1.90. The results tend to confirm those obtained from the microscopic observations (Table 7). In addition, the fractal dimensions observed for the control samples (I) were very close to those characterizing the corresponding reference samples, in particular for I1, I3 and I4.

The fractal dimensions characterizing the R aggregates of type 2 (aggregates with crushed portions) varied between 1.66 (R5A) and 1.86 (R2), while the degraded aggregates (type 3) were often characterized by D values above 2. These values are significantly different from those generally accepted for the characterization of structures such as soot aggregates [39].

For most of the samples studied, the number of D measurements performed was relatively low (<15). The observed tendencies therefore require verification using a larger number of soot samples with more measurements per sample.

Chemical Analyses

Pyrolysis-GC—The pyrograms of the soot samples from liquid combustibles were characterized by the presence of a group of three peaks of average intensity, situated between 55 and 60 minutes. Otherwise, the samples from the liquid combustibles could all be differentiated by pyrolysis-GC with the exception of the following three groups:

• L3 (white spirit), L5 (unleaded gasoline) and L6 (diesel);
• L8 (turpentine), L17 (toluene) and L19 (solution of 4 PAH's in toluene) (Fig. 17); and
• L14 (ST paint thinner) and L18 (clear varnish).

It was interesting to note that the pyrogram of unleaded gasoline soot (L4) could be differentiated from that given by leaded gasoline soot (L5). Similarly, two-stroke motor oil (L15) could be differentiated from four-stroke motor oil (L20) by the same technique.

The pyrograms of the soot samples produced from plastic materials were generally richer than for analogous liquid combustibles thus facilitating their differentiation. In addition, the pyrogram of a plastic-based soot was found to be very close to that characterizing the parent material itself (ie. the pyrogram of the solid, unburned polymer) (Fig. 18). This result may be explained by the fact that unburned polymer fragments are found in soot deposits resulting from the combustion of plastic materials. Examination of the chromatographic profile from the pyrolysis of a plastic soot sample can therefore permit the rapid identification of the parent polymeric material.

All of the soot samples from plastic combustibles could be differentiated by pyrolysis-GC, even though the two PVC samples (P1 and P11) gave similar chromatographic profiles. This was also the case for the two forms of polyethylene: P2 (LDPE) and P7 (HDPE). On the other hand, the soot from the two polystyrene samples (P4 and P8) could be readily differentiated by this technique.

The pyrolysis-GC method permitted an efficient discrimination between soot from plastic combustibles and that produces from liquid fuels. A disadvantage with the technique is that at least 50 μg of soot is generally required. However, at most fire scenes, sufficient sample can normally be recovered from cold spots such as window glass fragments.

Gas Chromatography (GC-FID and GC-MS)—The gas chromatograms recorded for the soluble organic fraction of soot samples L1 (methylated spirits), L12 (model airplane fuel) and L16 (brake fluid) were identical to that recorded for a blank (background reference) sample and are not considered in this discussion. For all remaining soot samples, differences in chromatographic profiles permitted a classification into groups or families exhibiting common characteristics.
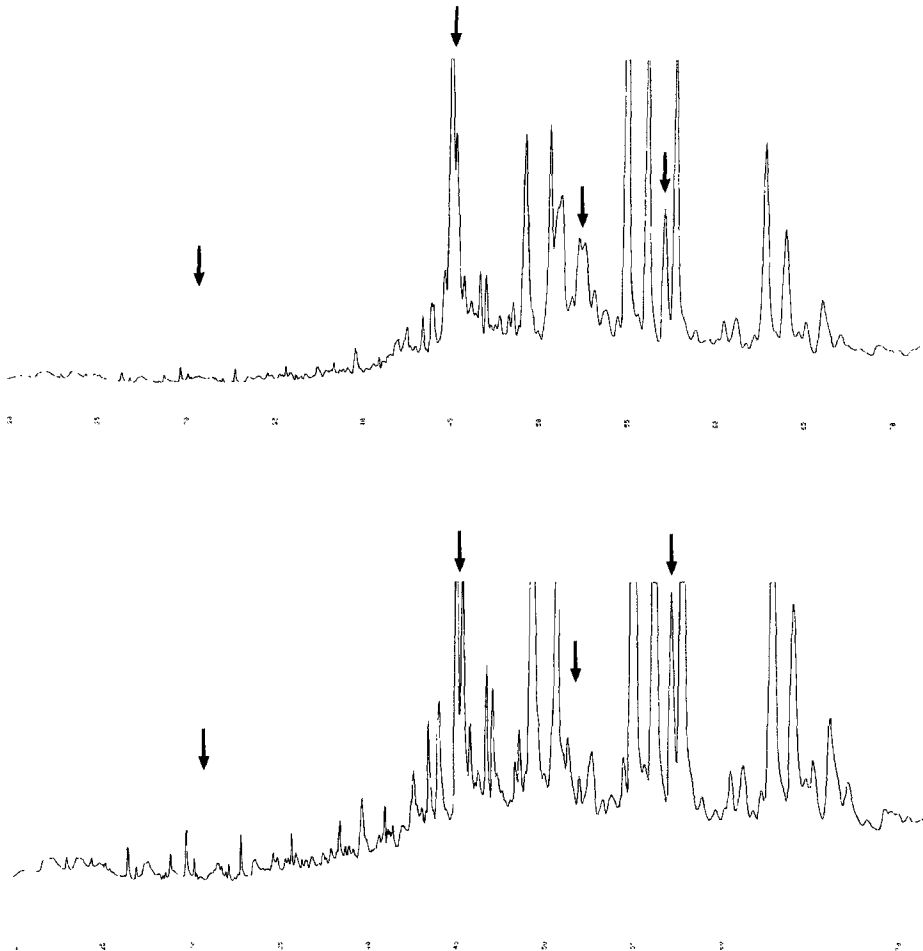
FIG. 17—*Comparison of pyrograms from the analysis of soot samples L17 (toluene; above) and L19 (solution of 4 PAH's in toluene; below). The quantitative differences indicated do not permit an unequivocal differentiation.*

a) Visual Comparison of Chromatograms.
The liquid-based soot samples could be placed into four distinct groups as follows:

• L4 (leaded gasoline), L8 (turpentine), L10 (paint thinner), L13 (CM paint thinner), L17 (toluene) and L19 (solution of 4 PAH's in toluene);
• L3 (white spirit), L5 (unleaded gasoline) and L6 (diesel);
• L14 (ST paint thinner) and L18 (clear varnish); and
• L2 (paraffin oil), L7 (kerosene), L9 (charcoal lighter fluid), L11 (paintbrush cleaner), L15 (2-stroke motor oil) and L20 (4-stroke motor oil).

Within a particular group, small variations were noted between each sample (principally quantitative differences) that were considered insufficient to permit an unequivocal differentiation (Fig. 19). It is of particular interest to note that the soot chromatogram for the leaded gasoline sample (L4) could be differentiated from that recorded for unleaded gasoline (L5).
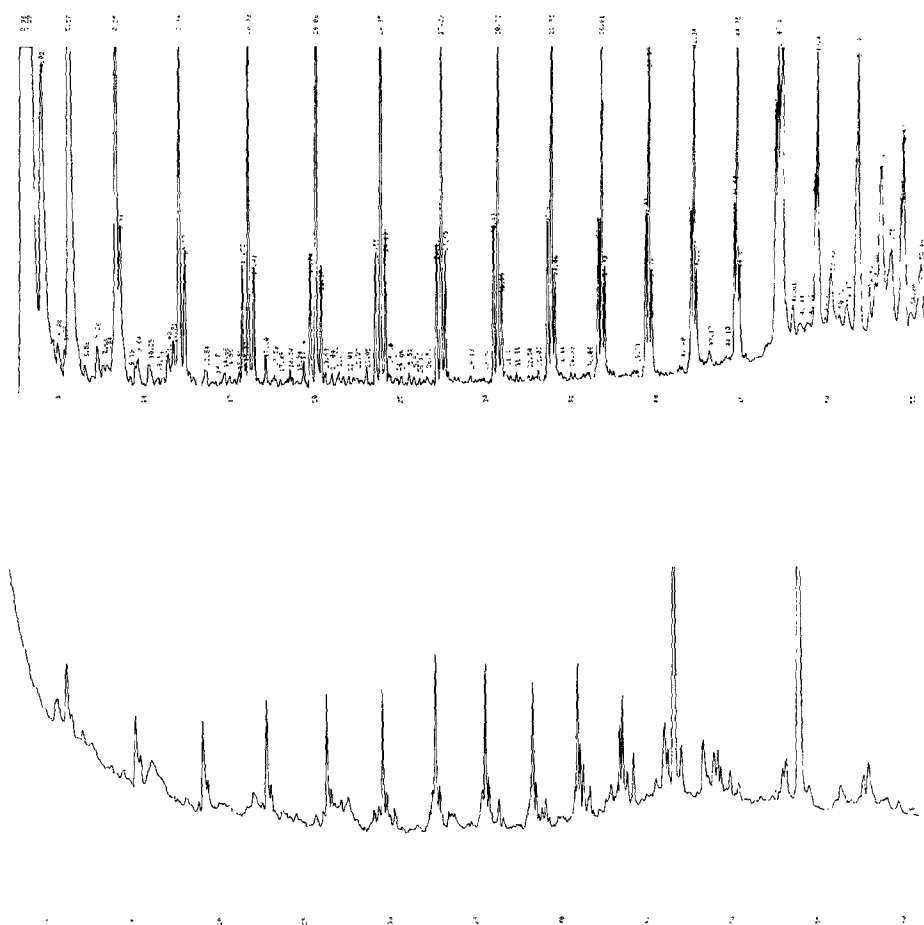
FIG. 18—*The chromatographic profile from the direct pyrolysis of a polyethylene sample (P2 = LDPE; above) is very similar to that obtained from the pyrolysis of a corresponding soot sample (P2; below).*

Compared to the corresponding pyrograms, the chromatograms from the plastic-based soot samples were more difficult to discriminate. Only samples P3 (PVC), P5 (PET), P6 (polyurethane) and P10 (carpet) could be clearly differentiated from the L samples and the remaining P samples. These remaining plastic soot samples gave chromatograms similar to some of the liquid-based soots and could be grouped as follows:

- P2 (LDPE), P7 (HDPE) and P12 (polyamide); and
- P1 (PVC), P4 (polystyrene), P8 (polystyrene), P9 (polypropylene) and P11 (PVC).

In no case could the chromatogram of a plastic-related soot be directly related to a particular polymer type (as was generally the case for the pyrolysis-GC analysis described above).

  b) Computer-Assisted Comparison of Chromatograms.

As discussed previously, a threshold value of 70 was found to be adequate for differentiation purposes (that is, MV ≥ 70 generally indicated non-differentiation). All of the L and P samples could be differentiated by this technique except for the following samples which were placed in four groups:
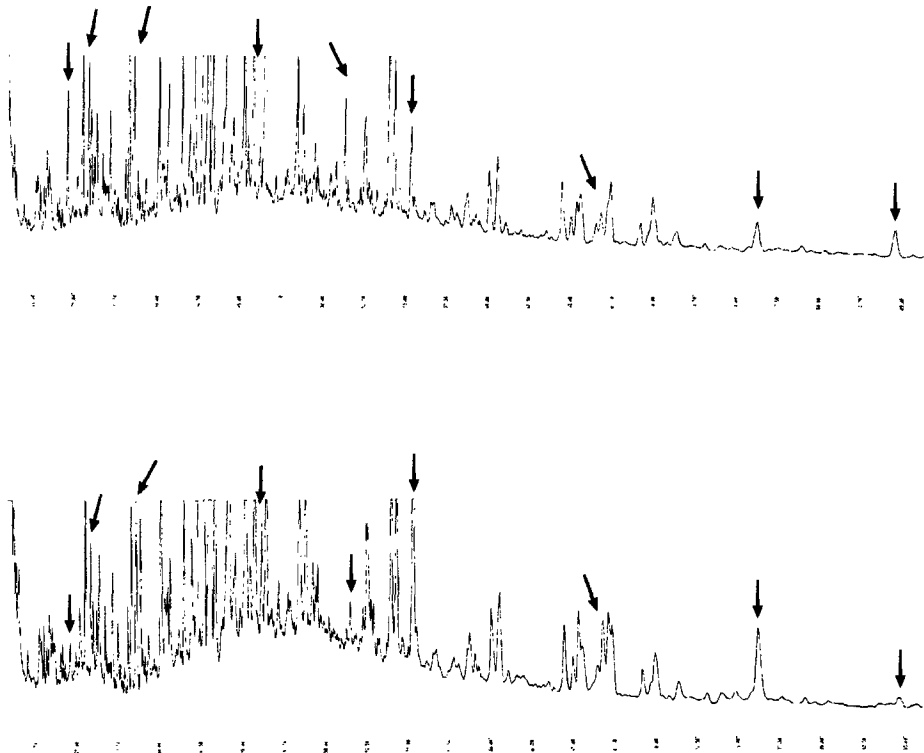
FIG. 19—*The chromatograms obtained from the soot samples L8 (turpentine; above) and L17 (toluene; below) show marked similarities. The differences are principally quantitative and do not permit an unequivocal differentiation.*

- L2 (paraffin oil), L7 (kerosene), L9 (charcoal lighter fluid), L20 (4-stroke motor oil), P7 (HDPE) and P12 (polyamide);
- L3 (white spirit), L5 (unleaded gasoline) and P3 (PVC);
- L8 (turpentine) and P8 (polystyrene); and
- L17 (toluene) and L19 (solution of 4 PAH's in toluene).

For the identification of liquid combustibles, the main dangers appear to come from the plastic materials P3, P7, P8 and P12, which gave results analogous to some of the liquid-based soot samples as indicated above. The chromatograms from weak smoke producers (L2, L7, L9, L20, P7 and P12) were all very similar. Likewise, the chromatograms from liquid combustibles rich in soot precursors (L17 and L19, for example) showed marked resemblances. It was noted, once again, that the chromatograms L4 (leaded gasoline) and L5 (unleaded gasoline) could be differentiated, as was also the case for L15 (2-stroke motor oil) and L20 (4-stroke motor oil).

The computer-assisted comparison of chromatograms (GC-auto) proved to be particularly efficient for the differentiation of the liquid-based soot samples and, in this respect, was complementary to the pyrolysis-GC procedure (which was more selective for the plastic soots). The identification of the plastic control samples (I3 and I4) proved to be particularly precise, with match values of 96 and 88 respectively (Table 9). In contrast to the reference samples, the control (I) samples from the combustion of liquid fuels were not clearly

TABLE 9—*Identification results obtained for the control (I) and casework (R) samples from each of the chemical methods employed. In each case, the corresponding reference samples have been placed in order of priority. ([1]GC-auto: match value $\geq$ 70; [2]GC-MS: results obtained from Fig. 4.)*

Sample	PY-GC	GC-Vis	GC-auto[1]	GC-MS[2]	Identity
I1	not analyzed	P12, L5, P10, L14, L7, L6, L18, L9, L3	P10, L14	L2, L7, P10	L5
I2	L14, L18, L3, L5, L6, L10, L15, L20	L7, L11, L20, P7, P12, L6, P1, P3, P5, P9	P12, L2	L20	L20
I3	P8, L8, L17, L19, L13, P4, P9	P8, P4, P1, L8, L17, L19, P9, P11	P8	P3, P4, P8	P8
I4	P9, P1, P11, P4, P8	P9, L8, L4, L10, L13, L17, L19	P9	P9	P9
I5	not analyzed	P7, L18, P12, L7, L9, L20, L2, L11, L14	L20, L2, L9, P7, L7	L2, L7, P10	L2
R1	P1, P11, L3, L5, L6, L14, L18, P2, P7	P2, P12, P7, L10, L4, L6, L11, L18, L7	—	L5	?
R2	not analyzed	L18, P7, L3, L6, L7, L11, L14, L5, L9, L20, P2, P3	L9, L20, L2	P6	?
R3	P2, P7, L3, L5, L6, L14, L18, L15	P12, L5, L18, P10, L7, L11, L14, L20, P7	P10, L14	L2, L7, P10	?
R4	L3, L5, L6, L4, L8, L17, L19, L10, L13, L14, L18, P4, P8	L8, L6, P11, L13, L17, L19, P1	—	L3	?
R5A	P2, P7, L3, L5, L6, L14, L18, P10, P1, P11	P2, P7, L3, L4, L6, L18, P3, P12, L7, L9, L11, L20	—	L18	?
R5B	P2, P7, L3, L5, L6, L14, L18, P1, P4, P3	L18, P2, P3, P7, L9	—	L18	?
R5C	P2, P7, L3, L5, L6, L14, L18, P10, P1, P11	P7, L13, L18, P2, L3, L4, L5, L6, L9, L20	—	L18	?
R6A	L3, L5, L6, P1, P11, P3, P6, P10	L4, L8, L13, L18, P4, P11, P5, P8, P1	—	L3	?
R6B	P1, P11, P2, P7, L3, L5, L6, P3, P6, P10	P7, P12, L2, L5, L7, L9, L11, L14, L20, P2, P6	L2, L5, P7, L7, L3, L15	L2, L7, P10	?
R7A	L3, L5, L6, L4, P1, P11, L14, L18, P2, P7, P9, P10	L5, P2, P6, L7, L11	P6, L7	L2, L7, P10	?
R7B	L3, L5, L6, L4, P1, P11, L14, L18, P2, P7, P9, P10	L5, L7, L9, L18	L9, L14, P7	L2, L7, P10	?
R8	L3, L5, L6, L4, L10, P2, P7, P10, L14, L18, P1, P11, P4, P9, L8	L6, P2, P7, L9	—	L3	?

identified by the GC-auto technique. This difference may be a result of the reduced combustion times employed for the preparation of the control samples.

Of the 12 casework soot samples analyzed by the GC-auto method, only 5 (R2, R3, R6B, R7A and R7B) gave concordances with match values higher than the threshold value (MV ≥ 70). As indicated in Table 9, the correlations given by the three chemical techniques pyrolysis-GC, GC-vis and GC-auto were often the same but in an order of priority (based on a probability of concordance) that was not always respected.

c) Search for Specific PAH Markers.

The principal qualitative differences between the different soot chromatograms proved to be with respect to the heavier, less volatile components. Unfortunately, the identification of these compounds, probably formed from various fused benzene structures, often proved difficult as they were present in limited quantities, close to the detection limit of the instrument employed.

The following PAH's were identified in most of the soot samples studied: acenaphthene (ACE), fluorene (FLUO), phenanthrene (PH), anthracene (AN), fluoranthene (FLUORAN), perylene (PER) and benzo[ghi]perylene (BghiPER) (Table 1). However, their relative concentrations, slightly higher for the rich soot samples, did not sufficiently vary for adequate differentiation. The compounds pyrene (PY), benzo[a]anthracene (BaAN), chrysene (CHRYS) and benzo[a]pyrene (BaP) appeared more selective, with concentrations that varied, sometimes quite significantly, from one soot sample to another. The samples exhibiting similar levels for each of these four PAH's are regrouped in Table 10. The groups have been composed of samples where the PAH levels (given as ng of PAH per kg of soot) vary between arbitrarily determined limits in each case. The BaP concentrations vary differently to those for the other PAH's and therefore these have been discussed separately.

i) Pyrene, benzo[a]anthracene and chrysene.

The medium to strong smoke producers L4, L6, L8, L10, L13, L17 and L19 gave the highest concentrations of pyrene, benzo[a]anthracene and chrysene. Samples L3 (diesel) and L5 (unleaded gasoline) both had similar PY, BaA and CHRYS levels which were significantly lower than for L4 (leaded gasoline); L4 and L5 could therefore be differentiated by this analysis. Samples L15 (2-stroke motor oil) and L20 (4-stroke motor oil) could also be readily discriminated; in fact, contrasting with L20, none of the three PAH markers in question were detected in the soot from L15 (as was also the case for L2, L7 and P10).

An interesting result was that the PAH concentrations were higher for the soot L17 (toluene) than for L19 (solution of four PAH's—phenanthrene, anthracene, fluoranthene and pyrene—in toluene). According to the literature [12], the presence of PAH's in the combustible should favor the formation of PAH's in the resulting soot. In our case, for the pyrene, which is present in the parent combustible L19, this has not been supported (nearly twice as much pyrene was detected in L17 compared to L19). The other PAH's are also more abundant in the soot sample L17. It has been shown that PAH's play an important role as precursors in the formation of soot and therefore are probably consumed or modified in the flames [36]. This implies that a high PAH concentration in the combustible does not necessary result in a high PAH concentration in the corresponding soot.

Concerning the soot from plastic materials, the samples P1/P3/P11 (PVC), and P4/P8 (polystyrene) gave the highest levels of PY, BaAN and CHRYS. While pyrene appeared to be the most abundant of the four PAH's for the liquid samples studied, the plastic samples were generally characterized by a high chrysene content, particularly in the case of P11, but also for P1 and P4.

ii) Benzo[a]pyrene.

Benzo[a]pyrene (BaP), without doubt the most studied carcinogenic PAH in natural systems, appears to be specific to certain types of soot and, in particular, soots produced from liquid combustibles. The concentration of BaP, in decreasing order, was as follows: L8 > L4 > P9 > L13 > L3 > L17 > P7 > P1 > L19 > P2 > L15. BaP was not detected

TABLE 10—*Classification of the analysed soot samples on the basis of their selected PAH content (PY = pyrene, BaAN = benzo[a]-anthracene, CHRYS = chrysene, and BaP = benzo[a]pyrene).*

PAH	PAH concentration (ng per kg of soot)				
	Not detected	< 500	500–1000	1000–4000	> 4000
PY	L2, L7, L11, L15, P7, P10, P12, I1, I2, I5, R3, R6B, R7A, R7B	P6, R2, R4, R6A	L3, L5, L14, P1, P2, R8	L4, L6, L9, L13, L18, L19, L20, P3, P4, P5, P8, P9, P11, I2, I3, I4, R5A, R5C	L8, L10, L17, R1, R5B
BaAN	L2, L7, L14, L15, L18, P6, P7, P10, P12, I1, I5, R2, R3, R5A, R5B, R5C, R6B, R7A, R7B	L3, L5, P5, P9, R1, R4, R6A	L20, P2, I2, I4, R8	L4, L9, L10, L11, L13, L19, P3, P4, P8, P11	L6, L8, L17, P1, I3
CHRYS	L2, L7, L14, L15, P10, P12, I1, I5, R2, R3, R6B, R7A, R7B	L3, L5, L6, L9, L11, L18, L20, P2, P6, P7, R4, R5A, R5B, R5C, R6A, R8	L4, I2, R1	L8, L10, L13, L17, L19, P1, P3, P4, P5, P8, P9, I4	P11, I3
BaP	L2, L5, L6, L7, L9, L10, L11, L14, L18, L20, P3, P4, P5, P6, P8, P10, P11, P12, I1, I2, I3, I5, R1, R2, R3, R5A, R5B, R5C, R6B, R7A, R7B	L15, L17, L19, P1, P2, P7, R4, R6A, R8	L3, L13, P9, I4	L4, L8	

in any of the remaining reference samples. In contrast to the other PAH's studied, BaP does not appear to be exclusively linked to the richer soot samples.

It is interesting to note that BaP was detected in only one of the PVC samples (P1), while being present in both of the polyethylene soots (P2 and P7). The concentration of BaP in P7 (LDPE) corresponds to approximately 8 times the level measured for P2 (HDPE). The P9 soot (polypropylene) presented the highest BaP level for all of the plastic samples, but this was still less than half that recorded for L8 (turpentine).

As indicated in Fig. 20 (dichotomic table), the specific concentrations of PY, BaAN, CHRYS and BaP permitted the unequivocal differentiation of all of the reference samples (L and P) except for the following, which could be placed in four distinct groups:

- L2 (paraffin oil), L7 (kerosene) and P10 (carpet);
- L13 (CM paint thinner) and L19 (solution of 4 PAH's in toluene);
- P3 (PVC), P4 and P8 (two forms of polystyrene); and
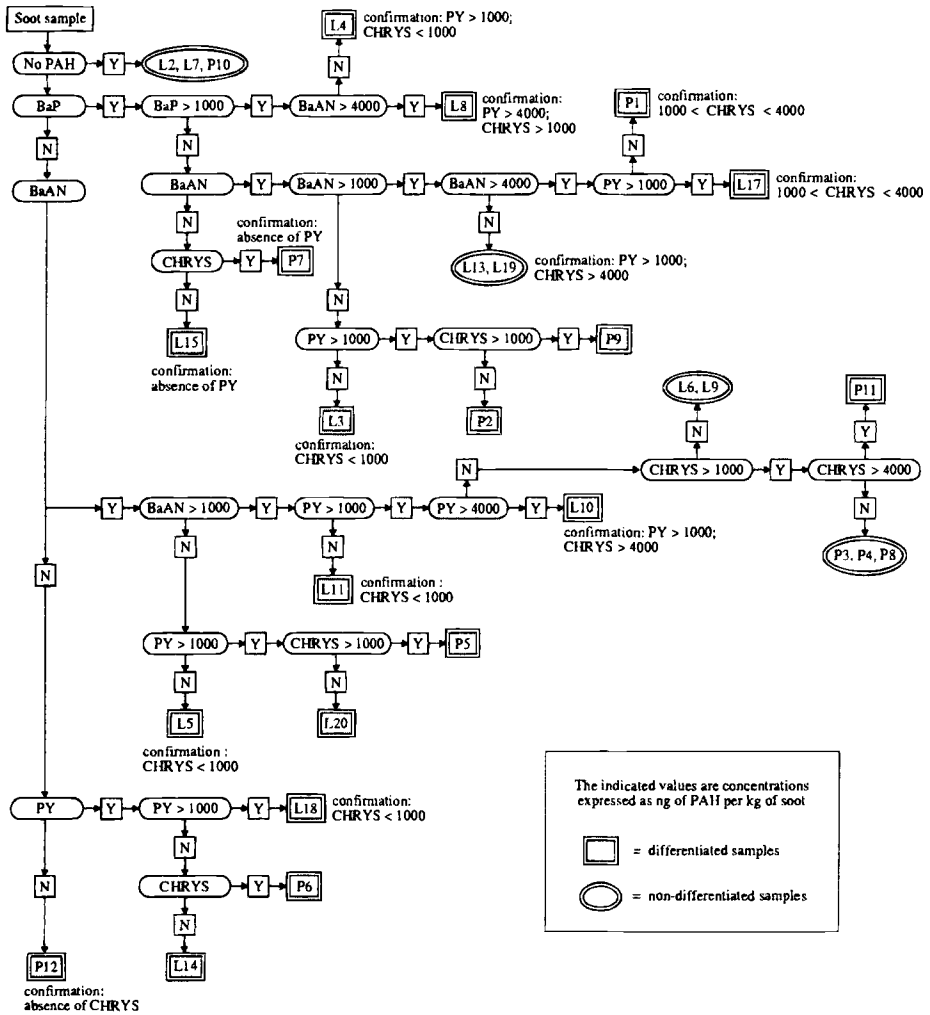- L6 (diesel) and L9 (charcoal lighter fluid).

FIG. 20—*Dichotomic table established on the basis of the analysis of 4 selected PAH's (PY = pyrene, BaAN = benzo[a]anthracene, CHRYS = chrysene, and BaP = benzo[a]pyrene) for the reference soot samples L (liquid fuels) and P (plastic combustibles).*

The identification of the I (control) and R (casework) samples was effected with the aid of the dichotomic table in Fig. 20. Control samples I2 and I4 were successfully identified by their PAH content. Sample I3 could not be differentiated from P3 (PVC) or from P4 and P8 (two forms of polystyrene). None of the four target PAH's were detected in the control samples I1 and I5.

The results obtained by the chemical analyses of the reference soot samples (L and P) have been summarized in Table 11. The identification of the control and casework samples, based on the results obtained from the reference soot deposits, is presented in Table 9.

Discussion

Macro- and microscopic observations can provide useful information on the type of soot in a particular deposit and on the presence or otherwise of structures such as polymer

TABLE 11—*Summary of the results obtained by the chemical analyses performed on the reference soot samples (L and P).*

Technique employed	Differentiated samples	Non-differentiated samples
PY-GC	L4, L10, L13, L15, L20, P1, P2, P3, P4, P5, P6, P7, P8, P9, P10, P11, P12	[L3, L5, L6] [L8, L17, L19] [L14, L18]
GC-Vis	P3, P5, P6, P10	[L2, L7, L9, L11, L15, L20, P2, P7, P12] [L3, L5, L6] [L14, L18] [L4, L8, L10, L13, L17, L19, P1, P4, P8, P9, P11]
GC-auto	L4, L6, L10, L11, L13, L14, L15, L18, L20, P1, P2, P4, P5, P9, PL10, P11	[L2, L7, L9, L20, P7, P12] [L3, L5, P3] [L8, P8] [L17, L19]
GC-MS (4 PAH's)	L3, L4, L5, L8, L10, L11, L14, L15, L17, L18, L20, P1, P2, P5, P6, P7, P9, P11, P12	[L2, L7, P10] [L13, L19] [P3, P4, P8] [L6, L9]

fragments (non-pyrolyzed particles) and characteristic soot forms. Such soot forms were particularly evident in samples from the combustion of PVC, polyethylene, PET and polyamide (nylon).

The results indicate that parameters associated to the size and the form of soot aggregates cannot be used for discrimination purposes. In fact, the morphology and the structure of soot aggregates which have suffered from major degradation (as was the case for most of the casework samples studied) are significantly different from those characterizing laboratory-prepared samples; their comparison is therefore difficult, if not impossible. As the variables employed for the discriminant analysis are all dependent on the size and the form of the soot aggregates, the results were found to be equally unusable in this case.

In addition, this analysis did not permit the correct identification of the control samples, even those composed of typical aggregates. These latter structures are generally formed from quasi-spherical "elementary particles," more or less compressed and reunited as clusters or in the form of chains. Such structures are often quite transitory. As the work of Arora [5] has shown, only soot samples produced under strictly controlled laboratory conditions permit the identification of the combustible, and then only for certain combustibles in particular.

The fractal dimension is a parameter that is, by definition, independent of the form of the particle analyzed. Measurement of this value for soot aggregates permitted the separation of rich soots (from the combustion of medium to strong smoke producers) from samples coming from weak smoke producers.

The results obtained from the chemical study of laboratory-prepared soot samples (by pyrolysis-GC, GC-FID and GC-MS) confirmed those obtained by physical methods. The differentiation of soot samples appears to depend on the composition of the parent combusti-

ble with respect to certain soot precursors (principally aromatic components) rather than on the chemical composition as a whole.

If sufficient sample is available in the soot deposit (at least 50 μg), the pyrolysis-GC technique is the method of choice, with a relatively high discriminating power, especially for soots resulting from the combustion of plastic materials. In these cases, the parent combustible can be generally identified due to the similarity between the soot pyrogram and that obtained from the pyrolysis of the unburned polymer. This technique may be of use in cases where a conventional accelerant analysis gives ambiguous results (ie. it may be unclear as to whether a particular chromatographic profile is due to the presence of a liquid accelerant or is simply the result of the pyrolysis of a plastic substrate).

If unsatisfactory results are achieved from the pyrolysis-GC analysis of a particular soot sample, or if insufficient material is available, then the soluble organic fraction (SOF) may be studied by GC-FID or GC-MS. This technique is more intricate as supplementary extract and purification steps must be performed.

The automatic comparison of soot chromatograms, using a simple computer program comparing the relative intensities of a number of selected components, may be used to confirm the results obtained by pyrolysis-GC or, in the case of soot samples from liquid fuels, provide additional classification information. Using the comparison algorithm described, two soot chromatograms were generally considered as being differentiated when a match value less than 70 was obtained (100 corresponding to a perfect match).

The search for selective PAH (polycyclic aromatic hydrocarbon) markers proved to be less successful than had been hoped and only partially agreed with results reported by Thatcher [4]. The following PAH's were identified in soot samples produced by the combustion of various petroleum derivatives: acenaphthalene, fluorene, phenanthrene, anthracene, fluoranthene, perylene and benzo[ghi]perylene. These compounds were generally more abundant in the rich soot samples, but the quantitative variations proved insufficient for discrimination purposes. On the other hand, the concentration levels recorded for four additional PAH's (pyrene, benzo[a]anthracene, chrysene and benzo[a]pyrene) proved to be more selective. A comparatively good discrimination was achieved when the relative concentrations for all of these four markers were taken into consideration. It must be noted, however, that only semi-quantitative values could be obtained in this study and that further verification, by more precise quantitative techniques, is required.

The complex nature of an uncontrolled fire significantly complicates such analyses as even small variations can lead to relatively large errors (as the measured PAH concentrations are typically quite low, close to instrumental detection limits). In a real fire situation, the "history" of a particular soot sample is generally unknown. A basic problem linked to the quantification of PAH's absorbed onto atmospheric particles such as soot is that these compounds undergo significant transformation (or decomposition) in the present of certain agents: for example SO_2, N_xO_y, ozone, sunlight, humidity and temperature [42,43].

The application of powerful quantitative techniques to the study of soot deposits would only be justified if the target compounds under study were sufficiently stable and specific for the combustible at the source of the fire. The search for specific markers in soot should probably be directed towards species other than the PAH's considered in this study. Sulfur compounds, for example, have proved useful in other areas for the identification of the combustion products from medium and heavy petroleum fractions [44,45]. It must be admitted, however, that the detection and quantitation of specific identification elements of this type often requires the application of complex analytical techniques.

The laboratory-produced soot samples, obtained by the combustion of various liquid and plastic materials, could be classified according to the results given by the physical (1 = macroscopic observations; 2 = microscopic observations; 3 = discriminant analysis; 4 = fractal dimension) and chemical analyses [5 = pyrolysis-GC; 6 = GC-FID with visual comparison of chromatograms (GC-vis); 7 = GC-FID with automatic comparison of chro-

matograms (GC-auto); 8 = GC-MS qualitative and quantitative study of selected PAH's]
(Table 12).

Soot samples from moderate to strong smoke-producing combustibles could be readily discriminated from those resulting from weak producers. This distinction was possible by a simple visual observation of the soot deposit using a macroscope, even though each subsequent technique provided the same information. For the combustibles classed as weak soot producers [methylated spirits (L1), heavy petroleum distillate (L2), kerosene (L7), scale model fuel (L12) and brake fluid (L16)] no subsequent discrimination was possible; these soots showed limited characteristics and the analytical methods chosen did not detect any exploitable differences.

The soot from moderate to heavy smoke producers could be further subdivided into liquid combustibles and plastic materials. The subclassification of these samples was possible with the aid of methods 1, 2, 6, 7, 5 and 8 (given in the order of increasing discriminating power); with the exception of method 6, these techniques permitted a final individual identification in most cases. The complete sequence of methods exhibited a high discriminating power (DP) and the information obtained from each individual technique was often complementary. Consequently, the results obtained from a combination of these tests increases the probability of an identification, as indicated in the corresponding dichotomic table (Figure 21). This table was constructed by taking into consideration all of the results obtained from the study of the laboratory-prepared (L, P and I) and casework (R) soot samples. Most of the samples examined could be differentiated on the basis of this table. Nevertheless, the results require confirmation and completion with information obtained

TABLE 12—*Comparison of the techniques employed in this study for the analysis of soot deposits (DP = relative discriminating power).*

| No.	Method	DP	Advantages	Disadvantages
1	Macroscopy: visual comparison	low	non-destructive; direct observation	limited information obtained
2	TEM: visual comparison	low	non-destructive	micrograting sampling technique required
3	Discriminant analysis	low	non-destructive; automatic procedure	depends directly on 2
4	Image analysis: fractal dimension	medium	non-destructive; automatic procedure	depends directly on 2
5	Pyrolysis-GC: visual comparison	high	rapid, simple to apply; reproducible results	destructive; requires > 50 μg soot
6	GC: visual comparison	medium	very sensitive; reproducible results	destructive; extraction procedure required
7	GC: computer-assisted comparison	high	very sensitive; reproducible results; automatic procedure	destructive; extraction procedure required
8	GC-MS: identification of selected PAH's	high	very sensitive; reproducible results; automatic procedure	destructive; extraction procedure required
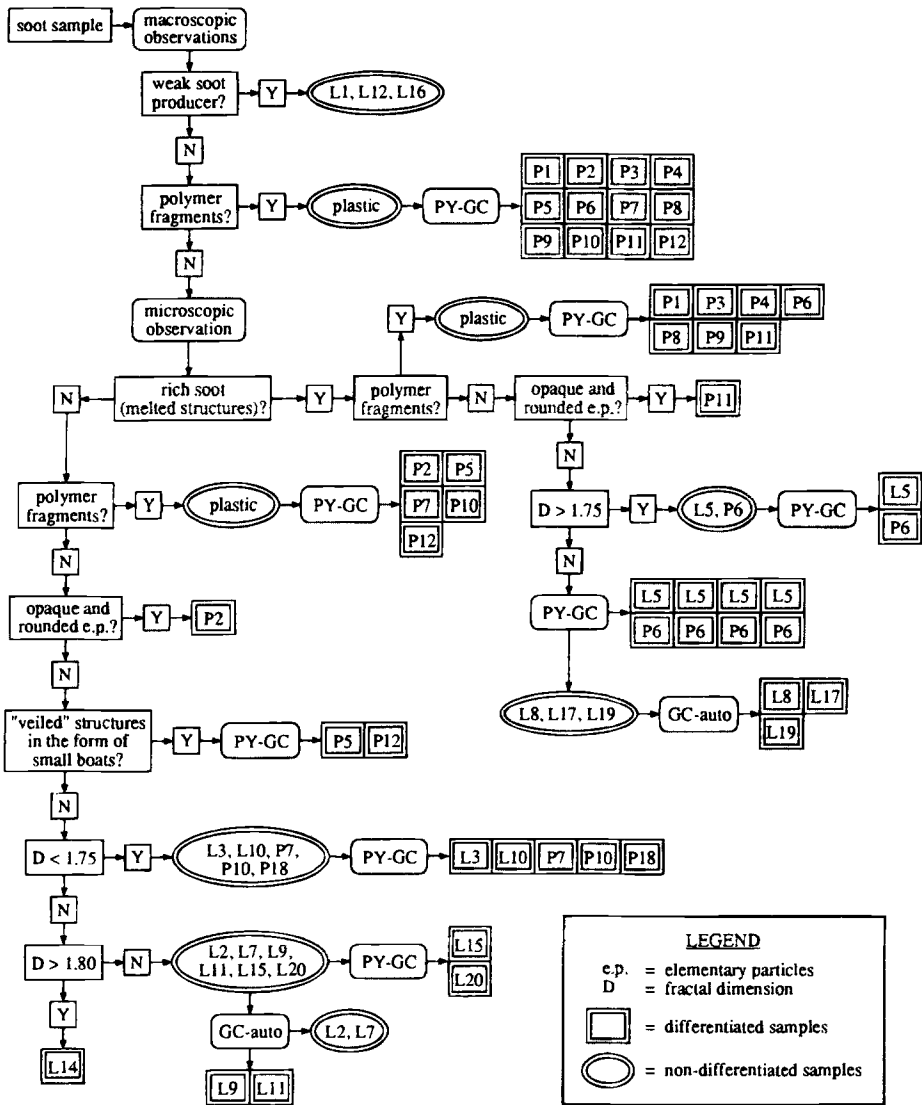
FIG. 21—*Dichotomic table established on the basis of the results obtained from physical and chemical analyses of soot samples L, P, I and R.*

from the study of a larger, more significant number of soot samples from casework fire scenes.

Conclusions

This study has indicated that the analysis of soot deposited on cold surfaces in the course of a fire (on window glass, for example) may provide useful information regarding the type of combustible involved. Only a limited number of cases have been examined but it is possible to conclude that this approach may:

• confirm the results obtained by classical techniques in positive cases (ie. where an accelerant has been detected), but also provide valuable information in difficult cases where identification of the combustible is not possible (for example, when the combustible at the seat of the fire has been totally destroyed or significantly contaminated);

• rapidly identify the presence of plastic materials in the combustible charge that tend to perturb conventional accelerant analyses;

• differentiate certain closely related products such as leaded and unleaded gasoline, two-stroke and four-stroke motor oil, etc.

However, the factors that may influence the state of a soot sample during a fire are numerous and largely unknown. These elements include the combustion conditions (duration, intensity, temperatures reached, etc.), atmospheric conditions (rain, wind, etc.), and destructive effects (from the fire itself, or due to fire-fighting techniques such as the use of water jets). All these factors, combined with the complex nature of the combustible mixture itself, lead to changes in the soot deposit that cannot be evaluated. As a fire develops, changes also occur in the fuels themselves; this must also result in variations in soot type and composition. A more detailed study of both laboratory and casework soot samples is therefore required to determine if the results from physical and chemical analyses, as presented in this work, have any significant value in fire investigations.

Acknowledgments

References

[1]   Caddy, B., Smith, F. P., and Macy, J., "Methods of Fire Debris Preparation for Detection of Accelerants," *Forensic Science Review,* Vol. 31, No. 1, June 1991, pp. 57–69.

[2]   Dietz, W. R., "Physical Evidence Of Arson: Its Recognition, Collection and Packaging," *Fire and Arson Investigator,* Vol. 41, No. 4, 1991, pp. 33–39.

[3]   DeHaan, J. D., and Bonarius, K., "Pyrolysis Products of Structure Fires," *Journal of the Forensic Science Society,* Vol. 28, 1988, pp. 299–309.

[4]   Thatcher, P. J., "The Scientific Investigation Of Fire Causes," In *Forensic Science Progress* (A., Maehly, and R. L., Williams, Eds.), Springer Verlag, Berlin—Heidelberg—New York—Tokyo, Vol. 1, 1986, pp. 117–151.

[5]   Arora, B. B., "Transmission Electron Microscopic Studies of Morphology and Crystallography of Particulate Emissions in Smokes," *Forensic Science International,* Vol. 32, 1986, pp. 185–192.

[6]   Carpenter, K. and Johnson, J. H., "Analysis of the Physical Characteristics of Diesel Particulate Matter Using Transmission Electron Microscope Techniques," *Society of Automotive Engineers,* SAE Paper No. 790815, 1979, pp. 2743–2757.

[7]   Capron, R. and Haymann, P., "Protocole pour une analyse quantitative des produits de combustion d'un fuel lourd par microscopie électronique," *Journal de Physique,* Vol. 24, No. 5, 1984, pp. 687–689.

[8]   Suzuki, N. and Ishiguro, T., "Observations of Soot in Automotive Engines," *Journal of Electron Microscopy,* Vol. 37, No. 5, 1988, p. 251.

[9]   Colbeck, I., "Dynamic Shape Factors of Fractal Clusters of Carbonaceous Smoke," *Journal of Aerosol Science,* Vol. 21, Suppl. 1, 1990, pp. S43–S46.

[10]   Mandelbrot, B. B., *The Fractal Geometry of Nature,* W. H. Freeman and Company, New York, 1983.

[11]   Feder, J., *Fractals,* Plenum Press, New York and London, 1988.

[12]   Haynes, B. S. and Wagner, H. G., "Soot Formation," *Progress in Energy and Combustion Science,* Vol. 7, No. 4, 1981, pp. 229–273.

[13] International Agency for Research on Cancer, *International Agency for Research on Cancer Monographs on the Evaluation of the Carcinogenic Risk of Chemicals to Humans, Vol. 35: Polynuclear Aromatic Compounds, Pt. 4: Bitumens, Coal-Tars and Derived Products, Shale-Oils, and Soots*, IARC, Lyon, 1985, pp. 219–245.

[14] Wheals, B. B., "The Practical Application of Pyrolytic Methods in Forensic Science During the Last Decade," *Journal of Analytical and Applied Toxicology*, Vol. 8, 1985, pp. 503–514.

[15] Takatsu, M. and Yamamoto, T., "Studies on Identification of Soots. I. Discrimination of Trace Amounts of Soot Produced from Combustion of Aromatic Hydrocarbons," *Nippon Kagaku Kaishi*, No. 10, 1988, pp. 1749–1752.

[16] Takatsu, M. and Yamamoto, T., "Identification of Soot. III. Identification of Soot Produced from Aromatic Hydrocarbon by Pyrolysis GC," *Bunseki Kagaku*, Vol. 38, No. 9, 1989, pp. 449–453.

[17] Salzman, B. E. and Berg, W. R., "Air Pollution," *Analytical Chemistry*, Vol. 49, 1977, pp. 1R–16R.

[18] Vorhees, K. J., Schulz, W. D., Kunen, S. M., Hendricks, L. J., Currie, L. A., and Klouda, G. A., "Analysis of Insoluble Carbonaceous Materials from Airborne Particles Collected in Pristine Regions of Colorado," *Journal of Analytical and Applied Pyrolysis*, Vol. 18, No. 3–4, 1991, pp. 189–205.

[19] Lee, M. L., Novotny, M., and Bartle, K. D., *Analytical Chemistry of Polycyclic Aromatic Compounds*, Academic Press, London, 1981.

[20] Jaklin, J., Krenmayr, P., and Varmuza, K., "Polycyclische Aromatische Verbindungen in der Atmosphäre von Linz (Oesterreich)," *Fresenius Zeitschrift für analytische Chemie*, Vol. 331, No. 5, 1988, pp. 479–485.

[21] Bingham, E., Trosset, R. P., and Warshawsky, D., "Carcinogenic Potential of Petroleum Hydrocarbons. A Critical Review of the Literature," Journal of Environmental Pathology, Toxicology, and Oncology, Vol. 3, No. 1–2, 1979, pp. 483–563.

[22] Di Lorenzo, A., Polletta, A., Ciccioli, P., Brancaleoni, E., and Cecinato A., "Emission of PAH from a Light-Duty Diesel Car As a Function of the Engine Operating Conditions: A Possible Approach for Investigating the Parameters Affecting Formation of Toxic Components in Soot," In *Polynuclear Aromatic Hydrocarbons: Measurements, Means, and Metabolism. Eleventh International Symposium on Polynuclear Aromatic Hydrocarbons* (Cooke, M., K. Loening, and J., Merritt, Eds.), Battelle Press, Columbus, 1991, pp. 239–258.

[23] Risner, C. H., "Benzo[a]pyrene in the Total Particulate Matter of Cigarette Smoke," *Journal of Chromatographic Science*, Vol. 26, No. 3, 1988, pp. 113–120.

[24] White, K. L., Jr., "An Overview of Immunotoxicology and Carcinogenic Polycyclic Aromatic Hydrocarbons," *Journal of Environmental Science and Health*, Vol. 4C, No. 2, 1986, pp. 163–202.

[25] Glass, L. R. and Easterly, C. E., "Ranking of PAH Carcinogenic Potencies," *Polynuclear Aromatic Hydrocarbons: Measurements, Means, and Metabolism. Eleventh International Symposium on Polynuclear Aromatic Hydrocarbons* (M., Cooke, K., Loening, and J., Merritt, Eds.), Battelle Press, Columbus, 1991, pp. 341–355.

[26] Diercxsens, P., *Contribution à la connaissance des sources et de la dynamique de quelques polluants prioritaires organiques dans l'écosystème sol*, Ecole Polytechnique Féderale de Lausanne, Thesis No. 681, 1987, pp. 5–16.

[27] Hirschler, M. M., "Soot from Fires: I. Properties and Methods of Investigation," *Journal of Fire Science*, Vol. 3, No. 5, 1985, pp. 343–374.

[28] Hirschler, M. M., "Soot from Fires: II. Mechanisms of Soot Formation," *Journal of Fire Science*, Vol. 3, No. 6, 1985, pp. 380–414.

[29] Pasternak, M., Zinn, B. T., and Browner, R. F., "The Role of Polycyclic Aromatic Hydrocarbons (PAH) in the Formation of Smoke Particulate During the Combustion of Polymeric Materials," *Proceedings of the Eighteenth International Symposium on Combustion*, The Combustion Institute, Pittsburgh, 1981, p. 94.

[30] Mellottee, H., "Le principe de la dégradation thermique des matériaux et la naissance des fumées," *Revue Générale de Sécurité*, Vol. 26, p. 69.

[31] Pedersen, P. E. and Ingwersen, J., "Effects of Fuel, Lubricant, and Engine Operating Parameters on the Emission of Polycyclic Aromatic Hydrocarbons," *Environmental Science and Technology*, Vol. 14, No. 1, January 1980, pp. 71–79.

[32] Akhter, M. S., Chughtai, A. R., and Smith, D. M., "The Structure of Hexane Soot. I: Spectroscopic Studies," *Applied Spectroscopy*, Vol. 39, No. 1, 1985, pp. 143–153.

[33] Akhter, M. S., Chughtai, A. R., and Smith, D. M., "The Structure of Hexane Soot. II: Extraction Studies," *Applied Spectroscopy*, Vol. 39, No. 1, 1985, pp. 154–167.

[34] Goss, J. C., "Brake Fluid Is a Fire Hazard," presented at the 12th Meeting of the International Association of Forensic Sciences, Adelaide, Australia, October 1990.

[35] Schulz, N., *Fire and Flammability Handbook,* Van Nostrand Reinhold Company, New York, 1985.
[36] Pinorini, M. T., *La suie comme indicateur dans l'investigation des incendies,* (PhD thesis, University of Lausanne) Imprimerie Schori, Villard-Chamby, 1992.
[37] Tabachnik, B. G. and Fidell, L. S., *Using Multivariate Statistics,* 2nd Edition, Harper Collins Publishers, Inc., New York, 1989.
[38] Norusis, M. J., *SPSS Advanced Statistics User's Guide,* SPSS Inc., Chicago, 1990.
[39] Prado, G., Lahaye, J., and Haynes, B. S., "Soot Particle Nucleation and Agglomeration," *Soot in Combustion Systems and Its Toxic Properties,* (J., Lahaye, and G., Prado, Eds.), Plenum Press, New York, 1983, pp. 145–162.
[40] Crilly, A. J., Earnshaw, R. A., and Jones, H., *Fractals and Chaos,* Springer Verlag, Inc., New York, 1991.
[41] Weitz, D. A. and Huang, J. S., "Self-Similar Structures and the Kinetics of Aggregation of Gold Colloids," *Aggregation Gelation,* (F., Family, and D. P., Landau, Eds.) North-Holland, Amsterdam, 1984, pp. 19–28.
[42] Kamens, R. M., Guo, Z., Fulcher, J. N., and Bell, D. A., "Influence Of Humidity, Sunlight and Temperature on the Daytime Decay of Polyaromatic Hydrocarbons on Atmospheric Soot Particles," *Environmental Science and Technology,* Vol. 22, No. 1, 1988, pp. 103–108.
[43] Kamens, R. M., Guo, J., Guo, Z., and McDow, S. R., "Polynuclear Aromatic Hydrocarbon Degradation by Heterogeneous Reactions with Dinitrogen Pentoxide (N_2O_5) on Atmospheric Particles," *Atmospheric Environment,* Vol. 24A, No. 5, 1990, pp. 1161–1173.
[44] Ogata, M. and Fujisawa, K., "Gas Chromatographic and Capillary Gas Chromatographic/Mass Spectrometric Determination of Organic Sulfur Compounds (OSCs) in Sediment from Ports: Significance of These Compounds as an Oil Pollution Index," *Bulletin of Environmental Contamination and Toxicology,* Vol. 44, No. 6, 1990, pp. 884–891.
[45] Bombaugh, K. J. and Lee, K. W., "Fingerprinting Pollutant Discharges from Synfuels Plants," *Environmental Science and Technology,* Vol. 15, No. 10, October 1981, pp. 1142–1148.

Address requests for reprints or additional information to
Maria T. Pinorini
Institut de Police Scientifique et de Criminologie
Université de Lausanne
Place du Château 3
CH-1005 Lausanne, Switzerland